Building and characterizing a miniaturized laser amplifier

by

David Latorre Bastidas

Bachelor thesis in Physics
Faculty of Physics, Mathematics and Computer Science (FB 08)
at the Johannes Gutenberg-Universität Mainz
August 24, 2021

1. Examiner: Prof. Dr. Patrick Windpassinger
2. Examiner: Prof. Dr. Klaus Wendt

I hereby assure that I wrote this thesis myself. I did not use any other sources than the ones indicated and quotes are referred to as such.

Mainz, August 24. David Latorre Bastidas

David Latorre Bastidas
QUANTUM
Institut für Physik
Staudingerweg 7
Johannes Gutenberg-Universität D-55099 Mainz
dlatorre@students.uni-mainz.de

Table of contents

1. Introduction

In the second half on the 20th century, scientists began to conduct scientific experiments in space. For example, between 1973 and 1974 almost 300 experiments were conducted in Skylab [1], the first United States space station. To do so, experimental setups conceptualized for use on Earth, had to be adapted and qualified for space. Not only did scientists have to make the experiments stable enough to survive the harsh environmental influences (e.g. during the launch and reentry phase), but also fulfill the so-called Size, Weight and Power budget (SWaP) of the respective experimental setup. However, the ongoing development of miniaturized setups did not only benefit experiments conducted in space, but also enabled a broad range of field experiments. Recent examples for such experiments are a compact cold atom gravimeter for field applications [2] and a compact atom-interferometer gyroscope based on an expanding ball of atoms [3]. Many of those experiments were conducted by collaborations involving many universities and institutes. In the modern time of established networks and convenient connectivity, many recent questions of science are tackled by such collaborations, to gain a broader spectrum of knowledge, skills and manpower. Therefore, the ability to easily transport experimental setups from one research center to another is necessary.

Regarding space experiments in physics, many of them require miniaturized laser systems, which can produce high quality and high power beams, like the ultra-cold quantum gases in microgravity experiments taking place on the ISS [4]. The QOQI group at the Johannes Gutenberg University Mainz, in which this thesis was conducted, is currently involved on the MAIUS [5] and the BECCAL [6] projects with various German universities and research institutes. Those experiments study ultra-cold atoms and Bose-Einstein condensates in microgravity environments, where laser beam powers around 100-300mW are needed for cooling, guiding and manipulating atomic clouds. These experiments need to be conducted several times on the ground in order to test their stability, calibration, liability, etc. before being launched. Therefore, the groups need to transport setup elements from one place to another between the cooperation partners, testing the experimental setup using the real system optical powers.

In this thesis, a miniaturized laser amplifier system based on a tapered amplifier chip (TA) is presented, which can be used with any conventional low power laser source of 780nm wavelength. This system will provide a reliable source of laser light with power of minimum 100mW ex output fiber, equal to the real system requirements. Furthermore, it will feature convenient portability for potential transportation to any

project partners, using optical fibers in the input and the output of the setup. In this thesis, enough information is provided so that any Institute or organization can build its own modular miniaturized amplifier system.

It was decided to create a modular amplifier system, based on a tapered amplifier chip, in order to solve the lack of power in the generally used diode lasers, like external cavity diode lasers (ECDL) or distributed feedback lasers (DFB). A tapered amplifier diode amplifies an input optical signal using a semiconductor gain medium in a tapered region. Many commercial manufacturers sell these lasers with the amplifier already placed into the laser [7]. However, there is no possibility to detach the amplifier in case you only want to use the laser itself. Therefore, having a portable modular amplifier where any laser beam of an specific wavelength can be easily guided into the system is more practical, as one could amplify the seed beam power only when needed.

Regarding the structure of this thesis, the theoretical background of the tapered amplifier chip and the necessary devices, as well as the optical elements used in this amplifier setup are described in the next section *2. Basics*. First, the theory and basics of a tapered amplifier is explained, followed by the basics of an optical isolator and the behaviour of a beam coming out of an optical fiber. The basics and theory of the TA will help the reader to understand the characteristics of the amplified beam. Since the TA itself is very sensitive to back-reflected light, it is necessary to understand how a so-called optical isolator suppresses the reflected light and can be implemented into the setup. Following the description of the isolators working principle, an introduction into gaussian beam optics, especially the evolution of diverging and converging gaussian beams, is given. This can be later used to choose the correct parts to be used regarding the fiber coupling of the TA output beam.
The explanation and calibration of the setup is given in *3. Experimental setup*. Here, the actual setup of the optical amplifier system will be presented, followed by explaining the functions of the various setup elements. Then, the alignment process followed in order to couple the amplified beam into the output fiber is explained.
After that, the taken measurements are presented in *4. Results*. The results will be conducted for three different setup configurations, comparing each configuration to the results presented in the paper written by Jayampathi C. B. Kangara et al. [8], which used a similar setup configuration. First, the so-called free beam configuration results are shown. This configuration is compared with the results shown in [8] to check that the TA produced the expected amplification. Then, the results using the second configuration, version 1 (V1), are discussed, where the miniaturized setup was mounted and calibrated using the same fiber coupler in the input and the output of the setup [30]. Finally, the measurements taken using the third configuration, version 2 (V2), are explained, where the output fiber coupler featured the optimized lens focal distance calculated in section *3.5 Fiber coupler*[31].
Finally, the conclusions will be stated in *5. Conclusion*. Here the results are compared to the initial objective regarding output power and stability. Furthermore, thoughts about how to improve the stability of setup are also included.

2. Basics

In this chapter, the theoretical background needed to understand the optical elements used in the setup is presented. First, a brief explanation about the functioning of a tapered amplifier is explained and then the theory behind the amplification of the seed beam in the gain medium is discussed in detail. Finally, the physics behind an optical isolator is explained, followed by a discussion about gaussian optics with the focus on the beam size evolution after an optical fiber. This will be important in later parts parts of the thesis, where the miniaturized amplifier system will be set up.

2.1. Optical amplifiers: Tapered amplifier

An optical amplifier is a device that directly amplifies the input optical signal, without converting it before to electrical power. There are different ways of achieving such an optical amplification, such as using solid-state materials [9], doped fibers [10], etc.

Specifically, in the presented miniaturized setup a tapered amplifier (TA) [29] is used, which uses a semiconductor material in the tapered region to amplify the signal. The main advantage of using a tapered amplifier (TA) is the great amplification power that it has without losing much beam quality, due to the taper shape where the beam can expand. Furthermore, due to its structure and materials, the output beam mode is the same as the seed beam mode. Finally, to have an idea of the amplification power that a TA can achieve, an amplification between 20 and 26 dB was obtained, using input powers of around 1 to 10 mW.

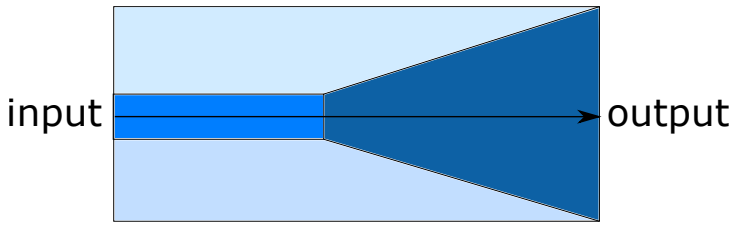

Figure 2.1.: Simplified setup of a tapered amplifier, where the dark blue region corresponds to the gain medium. The seed beam comes into the TA at the waveguide region, where a high energy density is achieved, and then the beam is amplified at the tapered region. Usually, there is also amplification in the waveguide region.

Regarding the shape of the TA itself two regions can be clearly distinguished, the output and the input (See Fig.[2.1]). The seed beam comes into the TA at the waveguide region, where a great power density is achieved. Then it goes to the taper region, where the amplification takes place. Due to its shape the beam can expand in this region maintaining a smooth amplitude envelope, obtaining a high quality beam in the output. Usually, there is also amplification in the waveguide region, where electrons are pumped e.g. via a separate electrode. Finally, the polarization of the seed beam affects the amplification in a semiconductor amplifier [14], where generally a transverse magnetic (TM) mode seed beam obtains more amplification than a transverse electric (TE) mode seed beam.

The typical measurement of the input aperture, width of the waveguide region, is around $1 - 5\mu m$ [8][11]. The output aperture depends on the angle of the tapered region, but for example in the used TA the output aperture was $210\mu m$ [11]. The input aperture is, therefore, about the same size as the MFD inside a single optical fiber [15] guiding light of 780nm wavelength. It is well-known how to couple light into a fiber and since the TA input aperture has the same size as the input fiber MFD, how to approach the TA coupling is known.

Further explanations about how the amplification takes place in the gain medium will be held in the next section.

2.2. Optical amplification in a semiconductor gain medium

In this section, the stimulated emission of a photon in a two level energy system is explained first. Then it is deduced how the population in the upper and lower level evolves when changing the energy difference between the two levels and also the temperature. Finally, how to get inversion of population, larger population in the upper level than in the lower level, adding a third level is briefly explained. The main purpose of this section is to understand how stimulated emission is produced and to connect the deduced results with the behaviour of a tapered amplifier.

First, it is considered that the gain medium has two energy-state levels, an upper one E_2 and a lower one E_1. An important consequence of this is having output power without an input beam, which is going to be discussed now. When the TA is connected to the current some atoms are excited from E_1 to E_2. The exited atoms decay to the lower one by spontaneous or stimulated emission, emitting a photon which energy will be the difference between the two energy-state levels (ΔE). Therefore, it is possible to have output power without an input beam by spontaneous emission.

The main problem of not using an input beam is that the input and output photons will not be coherent because the emission of the output photons will not be stimulated but spontaneous. However, if seed photons are used to stimulate the decay, output

photons will be coherent, conserving polarization, direction of propagation and frequency of the seed photons (See Fig.[2.2]).

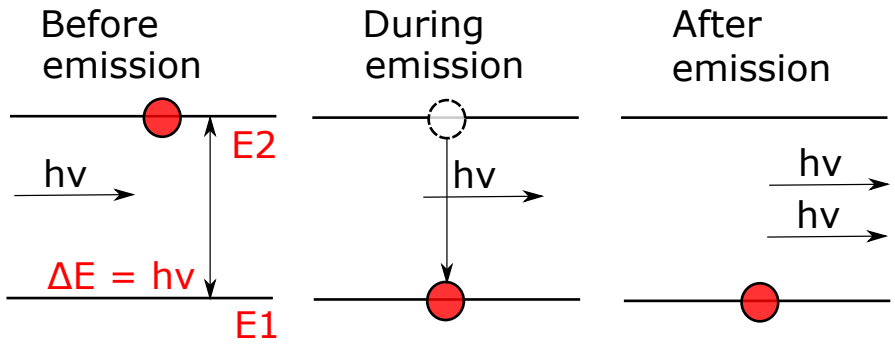

Figure 2.2.: Energy diagram that shows how stimulated emission works if considering a two energy level model. The incident photon stimulates the emission of another photon of energy $\Delta E = h\nu$. An atom is represented by a red dot.

To understand how the current put into the TA affects the output power, the Boltzmann distribution of a two energy level system is used. If no current is put into the TA, then the atoms will behave like the following equation [12]:

$$\frac{N_2}{N_1} = exp\left(\frac{-(E_2 - E_1)}{kT}\right) \tag{2.1}$$

Where N_2 is the number of atoms in the upper state and N_1 is the number of atoms in the lower state. Here, the atom population of each energy level only depends on the temperature of the system and the energy difference between the two levels.

However, when the mean energy of the medium is increased, the probability of finding an atom in the upper level also increases. For simplicity, the reference system where $E_1 = 0$ and $E_2 = \epsilon$ is used, where $\beta = 1/kT$. To calculate the probability of finding an atom in the upper or lower level, the so-called partition function is used [12], which is the sum of the Boltzmann factor of each energy level of the system:

$$Z = (1 + e^{-\beta\epsilon}) \tag{2.2}$$

The partition function used is the one from the canonical ensemble, that is used in statistical mechanics to describe a system in thermal equilibrium with a heat bath at constant T. In the setup this heat bath is the copper heat sink where the TA is placed (See Fig.[3.2]). Also, we consider that the total number of atoms in the system does not change. Furthermore, the measurements were taken at constant T, so the canonical ensemble is the one to be used here in order to explain the amplification in the TA.

The probability of finding an atom in one of the two states can be generally written as the Boltzmann factor of the level divided by the so-called partition function of the system:

$$P_1 = \frac{1}{1+e^{-\beta\epsilon}} \quad P_2 = \frac{e^{-\beta\epsilon}}{1+e^{-\beta\epsilon}} \tag{2.3}$$

Using a two energy level system, an inversion of population, $N_2 > N_1$, cannot be achieved. The maximum probability of finding an exited atom is 1/2, when $T \longrightarrow \infty$ or $\epsilon \longrightarrow 0$. Now, the equation (2.1) in our reference system is:

$$\frac{N_2}{N_1} = \frac{N * P_2}{N * P_1} = e^{-\beta\epsilon} \tag{2.4}$$

Again, it can be seen in (2.4) that there is no inversion of population in a two level energy system. Now, to understand how the current changes the probabilities of finding the electrons on each state, the equation of the mean energy of the described two energy level system must be discussed [12]:

$$\bar{E} = N\epsilon P_2 = \epsilon N_2 \tag{2.5}$$

Looking at equation (2.5) one can see that if increasing the mean energy of the system then the probability of finding an atom in the upper state also increases, as the number of atoms and the energy level difference remain constant. When the current applied into the TA increases, also increases the mean energy of the system and, therefore, the number of atoms in the upper level. Having more atoms in the upper energy level lead to more stimulated emissions, so more output power is achieved.

Finally, a three level system is briefly explained, which allows inversion of population. The inversion of population allows more stimulated emissions than a two level energy system as it allows N_2 to grow over 1/2, and therefore, more output power. The gain medium of the used TA features many energy levels.

In a three energy level system, the inversion of population can be achieved if having enough current (pump) and if the relaxation time (τ) in the transition between E_3 and E_2 is smaller than between E_2 and E_1. (See Fig.[2.3]). Then, when pumping atoms into the E_3 level from E_1, these exited atoms will decay fast to E_2, where this atoms take a slower time to decay to E_1, achieving inversion of population.
Using this model, the equation that describes the difference of atom population between E_2 and E_1, $N_2 - N_1$, is [13]:

$$\frac{N_2 - N_1}{N_{Total}} = \frac{(1-\beta)\eta W_p \tau_{rad} - 1}{(1+2\beta)\eta W_p \tau_{rad} + 1} \tag{2.6}$$

Where $\beta = \tau_{32}/\tau_{21}$, W_p is the transition probability between E_3 and E_1, τ_{rad} is the radiative decay rate between from E_2 to E_1 and η the so-called fluorescence quantum efficiency:

$$\eta = \frac{\tau_3}{\tau_{32}} \frac{\tau_{21}}{\tau_{rad}(2 \longrightarrow 1)} \tag{2.7}$$

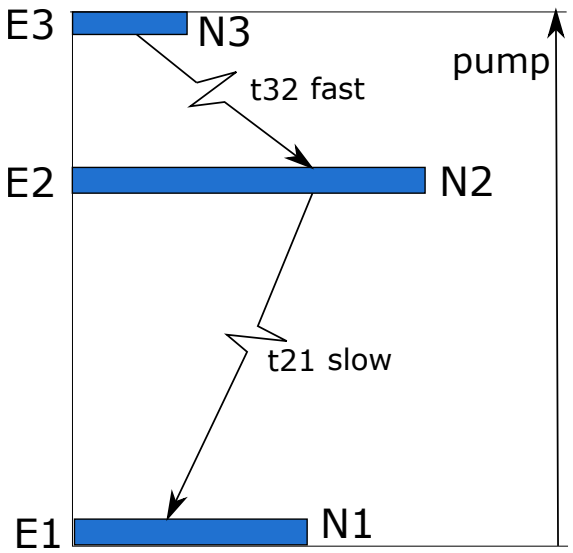

Figure 2.3.: Inversion of population in a three energy level system, where τ represents the relaxation time. The dark blue bars represent the number of atoms in each level.

Now, looking at equation (2.6), it can be seen that in order to achieve inversion of population, $\beta < 1$ is needed. Therefore, the relaxation time between E_3 and E_2 needs to be smaller than between E_2 and E_1.

Finally, knowing how stimulated emission works and how inversion of population is achieved, the basics of the amplification process in a tapered amplifier can be understood.

2.3. Optical isolator

An optical isolator is a device that allows light to pass in one direction but eliminates the light coming in the opposite direction. This feature is necessary in a TA based amplifier setup like the used one, as the TA is extremely sensitive to light retroreflections. The TA can be damaged when the back reflected photons get amplified and guided into the non tapered region. In the setup described in this thesis, for example, using an optical isolator was needed to avoid light retroreflections from the output fiber coupling.
In an optical isolator, to eliminate the light coming in the opposite direction a Faraday rotator is used, a device that applies a magnetic field to rotate the polarization of the beam, where the rotation angle is given by [16]:

$$\theta = \nu B d \tag{2.8}$$

Where ν is the Verdet constant [17], that depends on the material used, B is the applied magnetic field, and d is the distance that the light travels inside the Faraday rotator.
In the setup described in this thesis a Faraday isolator is used (polarization dependent isolator), which uses a Faraday rotator with $\theta = 45°$ and two polarizers, one in the input and the other one in the output of the rotator. A basic scheme is shown in Fig.[2.4].

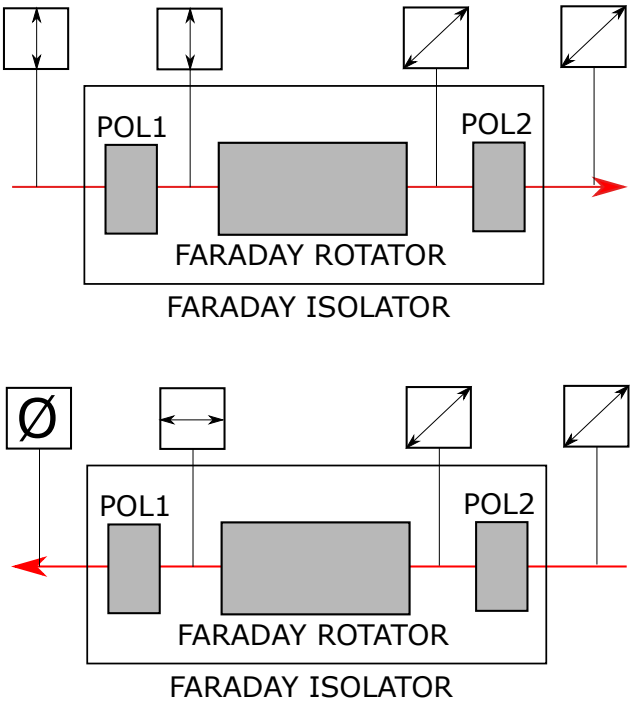

Figure 2.4.: Basic scheme of how the Faraday isolator allows light transmission in one direction but eliminates it in the opposite one. In the top scheme we can see how the beam coming in the forward direction is only rotated 45 degrees, as the polarization the beam has is the same as the polarizers. However, in the bottom scheme we see that the beam coming in the opposite direction is eliminated, as after the faraday rotator its polarization is perpendicular to the polarizer

Regarding the light beam in the forward direction, it will first go through to a 0° polarizer, then the light will be vertically polarized before going through the rotator. In Fig.[2.4] the input beam is a vertically polarized one, however, in the real setup only that the beam is a linearly polarized one is known, therefore it will be very important to match the incoming beam polarization with the 0° polarizer by rotating the isolator in order to optimize the isolator transmission (See Malus's Law (2.9)):

$$I = I_0 cos^2\alpha \tag{2.9}$$

In this equation, I_0 is the incident intensity and I the transmitted intensity after the isolator. This equation states that when an incident light beam crosses a polarizer, the intensity measured after the polarizer will depend on $cos^2\alpha$, where α is the difference between the angle of polarization of the input beam and the input polarizer .

After the input polarizer the light beam will be vertically polarized. Then, when going trough the rotator, the latter will rotate the polarization angle by 45°(2.8), which is also the angle of the output polarizer (analyzer).
About the beam coming in the opposite direction, its polarization will be 45° after the analyzer. In this case, knowing the polarization of this beam is not needed because its intensity after the isolator is expected to be zero, so it is not necessary to know its initial intensity. Then, when passing through the Faraday rotator, the beam will be horizontally polarized. Finally, when this beam goes through to the input polarizer (0°), its intensity will be zero as the polarization of the beam was perpendicular to the polarizer (See (2.9)).

2.4. Optical fiber

In the amplifier setup optical fibers are used in order to guide the seed beam into the amplifier and also to guide the amplified output beam. Therefore, the basics of its operation are here explained. Optical fibers are made from drawing glass or plastic, whereafter their width is comparable to the human hair [18]. Its operation is based on the total internal reflection principle, where the input light coming into the fiber propagates inside the fiber by multiple reflections.

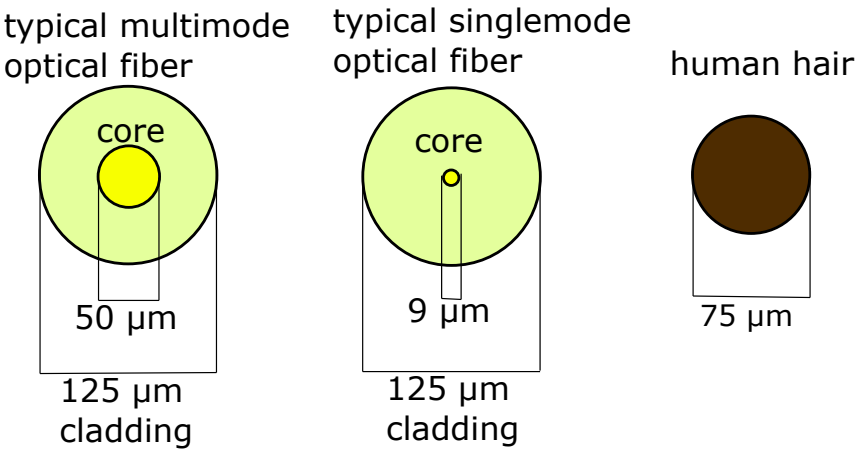

Figure 2.5.: Size comparison between typical multimode and singlemode fibers with a human hair

Regarding the typical structure of an optical fiber, they are usually composed by three layers: core, cladding and buffer [18]. The core is the region where the light propagates through the fiber by total reflection, usually made by pure glass. The cladding, which has a lower refraction index than the core, surrounds the core favouring the propagation of light inside the optical fiber. Finally, surrounding the cladding the buffer is found, which is usually made from plastic and protects the fiber from damages.

It is interesting to know the angle of the beam that comes in and out of the optical fiber, because in the used setup the lenses should be placed in the most optimal way in order to achieve a collimated light beam or to couple the beam into the fiber. To understand the basics, the numerical aperture (NA) of the optical fiber should be first explained, which is the sine of the maximum angle at which the ray that can reflect internally and, therefore, propagate inside the fiber.

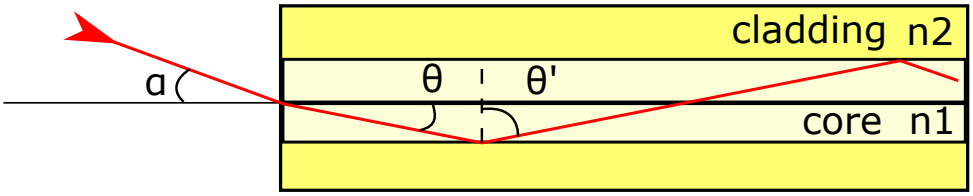

Figure 2.6.: Basic scheme of the light that will reflect into the fiber core. Where α represents the incident angle of a light beam coming into the fiber core. In this scheme, the refraction index (n) of the cladding is lower than the core one.

In order to deduce the equation for the NA, only applying Snell's law [19] twice is needed. Following the criteria used in Fig.[2.6]:

$$sin\alpha = n_1 sin\theta \tag{2.10}$$

Where n is the refraction index. Now it is considered the limit scenario where α is the maximum angle at which the ray propagates inside the fiber. Then, $\theta' = 90^{o}$:

$$n_1 sin\theta'_c = n_2 sin90 = n_2 \tag{2.11}$$

Finally, using both equations above, it is possible to determine the equation for the NA of an optical fiber.

$$NA = sin\alpha \overset{(2.10)}{=} n_1 sin\theta_c = n_1 sin(90-\theta'_c) = n_1 cos\theta'_c = n_1\sqrt{1-sin^2\theta'_c} \overset{(2.11)}{=} \sqrt{n_1^2 - n_2^2} \tag{2.12}$$

Therefore, if $n_1 = n_{core}$ and $n_2 = n_{cladding}$:

$$NA = \sqrt{n_{core}^2 - n_{cladding}^2} \tag{2.13}$$

In the setup, an optical fiber with $NA = 0.12$ is used, so the fiber does not permit the reflection of light inside the fiber if the incident angle is not lower than 6.9^{o}. Therefore, it was needed to select the right output fiber coupler to guide as much beam light as possible into the fiber with an angle lower than 6.9°.

Another aspect to think about is the divergence of the beam out of the fiber or analogue a focussed converging beam to be coupled into an optical fiber. In order to explain it, a gaussian beam inside a single mode fiber is considered. In the setup, a TEM_{00} gaussian beam was used as the seed beam, which beam profile is circular. However, the diameter of the beam inside the fiber is not the diameter of the fiber core itself but the Mode Field Diameter (MFD), which is usually slightly larger than the fiber core [20]. If guiding a gaussian beam with a certain diameter into the fiber using a lens that does not guide the beam into the fiber with the MFD, the transportation of light into the fiber will not be as efficient as it could be because the optical fiber only allows light to travel inside of it at the MFD. Thus, it was needed to choose wisely the fiber coupler lens focal distance to be able to focus the beam to the MFD of the fiber.

In order to explain how a gaussian beam evolves in the direction of propagation, it is considered that its minimum width is on the edge of the fiber and then it evolves as a gaussian beam in free space.

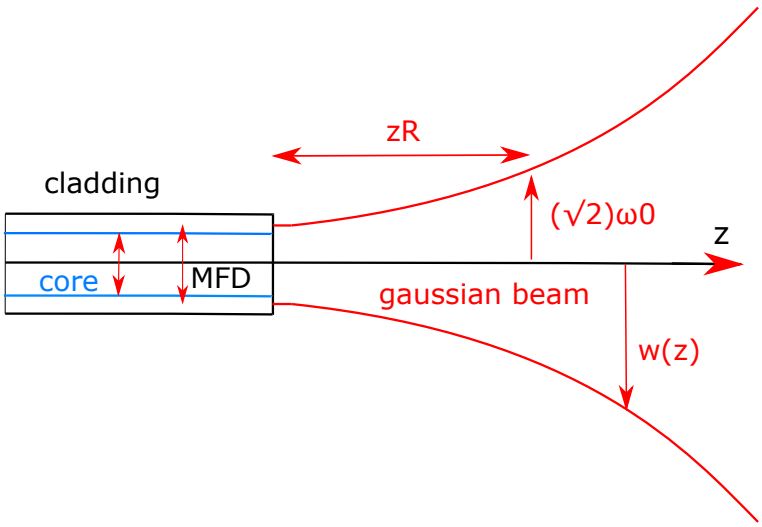

Figure 2.7.: Gaussian beam waist evolution in the direction of propagation when coming out of a fiber. Inside the fiber the beam diameter is not the core diameter but the MFD.

The beam waist evolution of a gaussian beam is given by the hyperbolic relation [22]:

$$\omega(z) = \omega_0 \sqrt{1 + (\frac{z}{z_R})^2} \tag{2.14}$$

where

$$z_R = \frac{\pi \omega_0^2}{\lambda} \tag{2.15}$$

In these equations ω_0 is the minimum width (radius) of the beam, therefore, in a gaussian beam coming of out a fiber, $2\omega_0$ will be equal to the MFD of the fiber. Also, as it can be seen in (2.15), there is a quantity defined as z_R (Rayleigh length), which is the distance in the direction of propagation at which the beam waist is equal to the minimum waist width multiplied by $\sqrt{2}$. This quantity, z_R, depends on π, λ and ω_0. Here λ represents the wavelength of the beam. Finally, from (2.14) and (2.15) one can see that the gaussian beam width evolution is directly proportional to the wavelength of the beam and inversely proportional to the initial width of the gaussian beam.

3. Experimental setup

In this chapter, the experimental setup used to create a miniaturized laser amplifier is explained. First, an introduction to every element is given, stating the model used and the manufacturer. Then, the placement of these devices into our setup is discussed. Finally, it is explained the alignment process used in detail in order to achieve the maximum efficiency possible using these components.

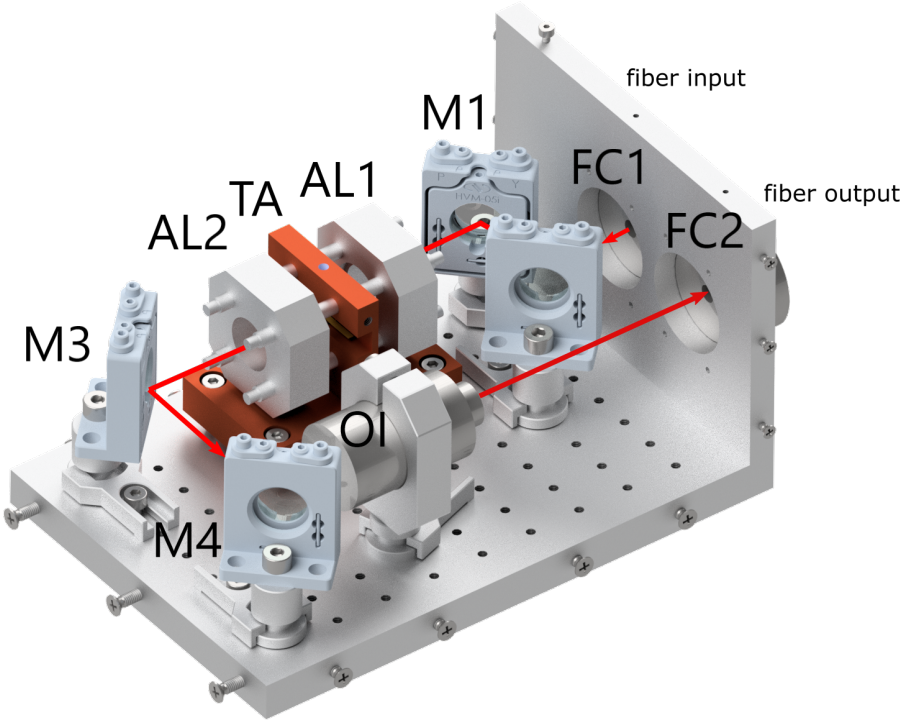

Figure 3.1.: Initial design, by Sören Boles [23], followed in order to build the tapered amplifier system (140x100x80mm). In the final design a cylindrical lens, which is not shown here but will be discussed, was used after the fourth mirror in the direction of propagation. FC: Fiber coupler; M: Mirror; AL: Aspherical lens; TA: Tapered amplifier; CL:cylindrical lens; OI: optical isolator. The list of the components used is shown in the Annex

In order to make this setup possible, the TA and all the lenses and devices were adjusted and aligned. The aim is to use this system to emulate laser power usually

used in space experiments, however, it can also be used in any lab if more laser power is required. Also, the reason behind building a miniaturized, resistant setup is to be easy to transport between laboratories without putting in risk the amplifier. The box designed by Sören Boles [23] is made from black anodized Aluminium in order to avoid damage by possible light reflections and unwanted electrical conduction. Finally, the inside box measurements are 140x100x80mm, therefore it was necessary to use miniaturized custom-made mounts and devices in order to fit them all inside the box.

The approach chosen in order to design the system was building a portable device that could amplify the power of a laser beam of 780nm wavelength. Therefore, it was thought to build a miniaturized box with an input and an output fiber coupler attached to an optical fiber, to have a user friendly amplifier system.

In general, such an optical amplifier system based on a TA needs the following components: a peltier element, a heat sink, thermistor, a laser diode controller, a tapered amplifier, a fiber coupler, an optical isolator, mirrors, aspherical lenses, a cylindrical lens and optional one or more waveplates. In the following, all these elements are briefly discussed. First, the used seed laser is discussed, explaining the advantages of using an ECDL in the setup. Then, the temperature control system is explained, constituted by a peltier element, a heat sink, a thermistor and a laser diode controller. After that, the main characteristics of the used TA are discussed. Finally, an explanation about the optical devices used and its alignment into our system is given.

3.1. The seed laser

An External Cavity Diode Laser (ECDL) made by Toptica Photonics is used for seeding the amplifier. Specifically the version DL pro-018064 [25], which produces a tuneable laser beam from 765 nm to 805 nm, however, in the setup the laser is used at 780 nm. Regarding the power of the laser, for this setup the seed laser is used at around 10 mW maximum optical power in order not to damage the TA.
An ECDL provides a laser beam with a small linewidth and a low phase noise. The main disadvantage is the lack of power that these type of laser diodes offer and that they are not very frequency/intensity stable. For the designed setup, not much optical power from the seed beam is needed, therefore it was decided to use an ECDL for seeding the system.

3.2. Peltier element and heat sink

The TA is extremely sensitive to temperature changes, as the output power depends directly on the temperature as seen in *2.2 Optical amplification in a semiconductor gain medium*. Thus, it is necessary to use a temperature controller system in order to

control the TA. In the setup, the Peltier element RC3-6 made by Marlow Industries Inc. [26] and a copper heat sink are used, as seen in Fig.[3.2]. Furthermore, it is also necessary to place a thermistor next to the TA inside the heat sink in order to monitor the temperature (and also for the temperature controller feeback loop).

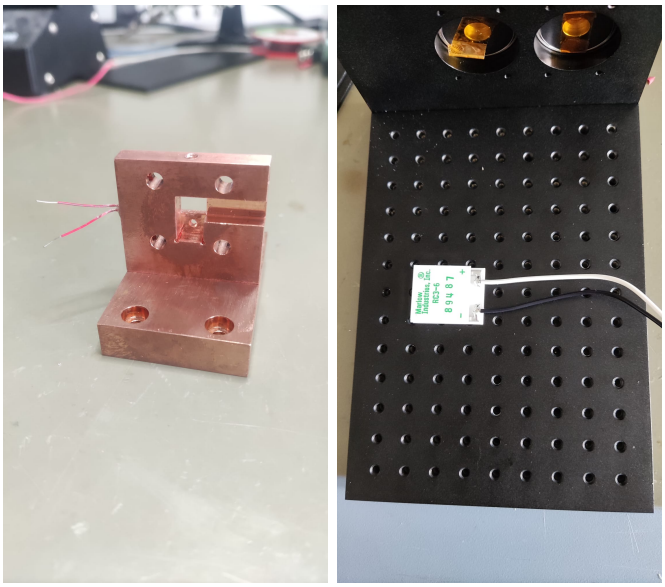

(a) (b)

Figure 3.2.: (a) Copper mount used as a heat sink. In the left side we can see the thermistor already placed in the mount. (b) Peltier element inside the box. The heat sink will be placed on top of the Peltier element.

While placing the thermistor inside the heat sink, it is critical not to use too much thermally conductive heat paste. The paste should only be used to fill the microscopic gaps between the thermistor and the heat sink. The reason is that the paste is not ideally conductive, therefore one would lose sensitivity while measuring the temperature. After placing the thermistor with the thermal paste, the thermistor was glued using UHU Endfest Plus 300, as the whole system need to be solid in order to get stable temperature measurements.

Regarding the heat sink, it is used a T-shape copper mount as seen in Fig.[3.2(a)]. Although the most important feature of the heat sink is the material used, it is also essential to chose a shape that allows a good heat flow. The copper mount used in this setup has a solid plate on the bottom that will be touching the Peltier element (see Fig.[3.4]). This allows an effective heat flow as the base of the copper block dissipates the heat due to its big size in comparison with the Peltier element device and the upper part of the heat sink, where the TA is placed.

Apart from achieving a constant temperature system, to take the measurements at 20°C was wanted in order to directly compare them with [8]. The laboratory temperature was around 25°C, therefore, the system needed to be capable of lowering the temperature of the TA at least 5°C. As seen in the Data Sheet of the peltier element [26], it is capable of achieving $\Delta T = 65$ at 27°C between the two sides of the peltier element. Therefore, this peltier element can be used in the system to achieve the wanted temperature, 20°C at 25°C.

3.3. Laser diode controller and cable setup

To control the parameters of the laser diode, the controller LDC-3744C [27] is used. This controller allows to control the temperature and the current put into the TA. In order to connect this controller to the box, two specifically soldered cables are used, one for the current and another one to control the temperature of the TA, which will be controlled by using a Peltier element.

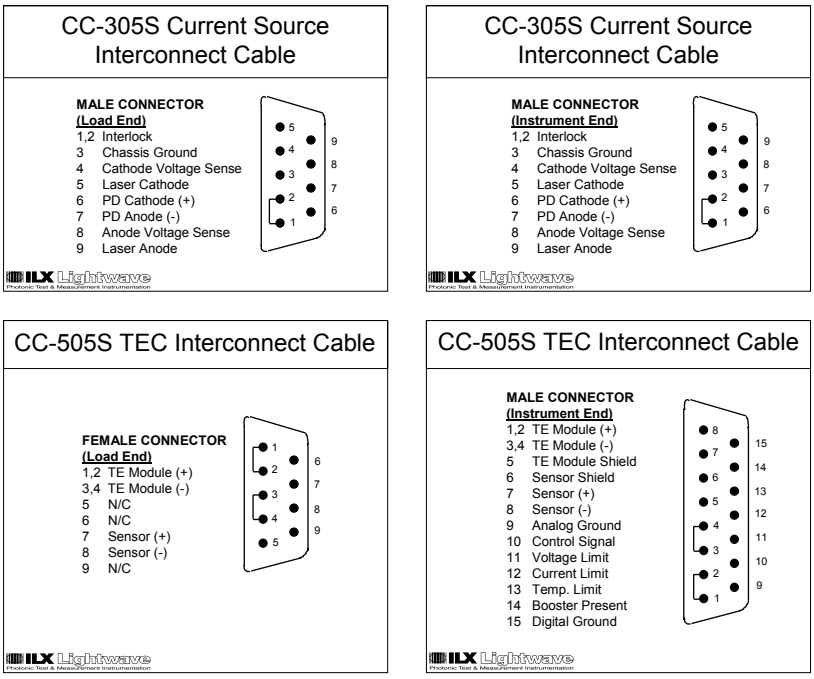

Figure 3.3.: Pinout diagram of the cables used in the controller [27]. On the left side there are the two D-subs connected to the system, and in the right side, the ones connected to the laser controller. From the left side pins, only the ones needed to control the temperature and the current of the TA were soldered.

The cables used are the CC-306S and CC-501S instead of the ones in Fig.[3.3], however, they are also valid. About the CC-306S, the Load End cables were manually soldered only to pins 5 and 9 and also an external cable to pin 7 for the +5V (security circuit) and another one to pin 6 for GND were soldered. Regarding the CC-501S, the Load End the TE+ cable was soldered to pin 1, the TE- one to pin 3 and both pins 7 and 8 to the corresponding cables. The rest of the Load End cables are not soldered to any pin.

In Fig.[3.4] it can be seen where the TA mount is placed inside the box (the Peltier element is just below the mount). The mount was screwed using plastic screws to avoid undesirable electrical conduction which could damage the tapered amplifier. It is hard to see where the cables go inside the box, but the thermistor was soldered to the proper cable. On the top side of the figure it is seen the security circuit used in order to avoid current peaks. The used handmade security circuit gives a delay on the input current to suppress harmful current spikes while switching the current on and off. Although, in Fig. [3.4] the TA is still not mounted, the only cable connection left is the cable that goes directly from the security circuit to the TA.

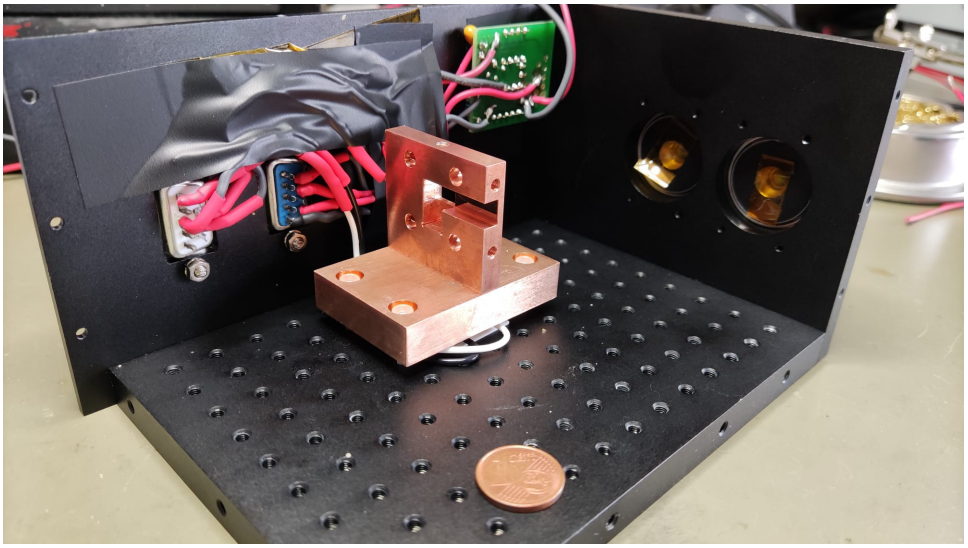

Figure 3.4.: The TA copper mount and the Peltier element already placed in the box with the proper cable connections. The security circuit can be seen on the top right side of the back plate. To give the reader an idea of the scale the amplifier setup, a 1 cent coin ($d = 16.25mm$[28]) was placed next to the copper mount.

3.4. Tapered amplifier

The tapered amplifier used is the 780nm 2W C-mount version from Eagleyard Photonics [29]. This TA should have an amplification of 22 dB at the recommended maximum forward current according to the manufacturer.

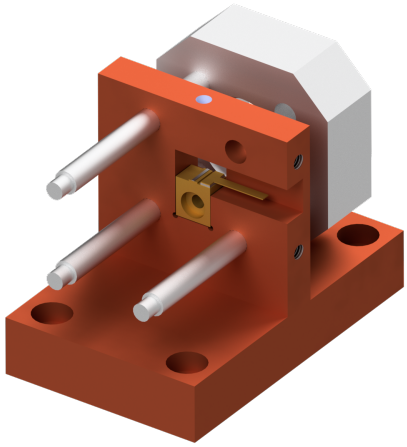

Figure 3.5.: Rendering of the C-mount TA placed inside the heat sink. At the back side it can be seen how the mount of the aspherical lens is mounted into the copper mount. An aspherical lens will be used at both sides of the TA in order to get a collimated beam and to couple the input beam into the TA waveguide.

Regarding the shape of the tapered region, one can clearly distinguish two regions, the input and the output (See Fig.[2.1]). About the input, this chip has a parallel angle of 23° while the perpendicular one is 40° (See Fig.[3.6]). The output beam shape is similar but not the same, whereas the perpendicular angle is also 40°, the parallel one is 18°. Due to the fact that the angle is not the same in both parallel and perpendicular axis, it is expected to only collimate one of the axis with a single aspherical lens. In the described setup, an aspherical lens is used to collimate the beam in the stronger divergent perpendicular direction, therefore, using a cylindrical lens to collimate the beam in the parallel direction after the aspherical lens of the output is recommended in order to get a circular beam profile.

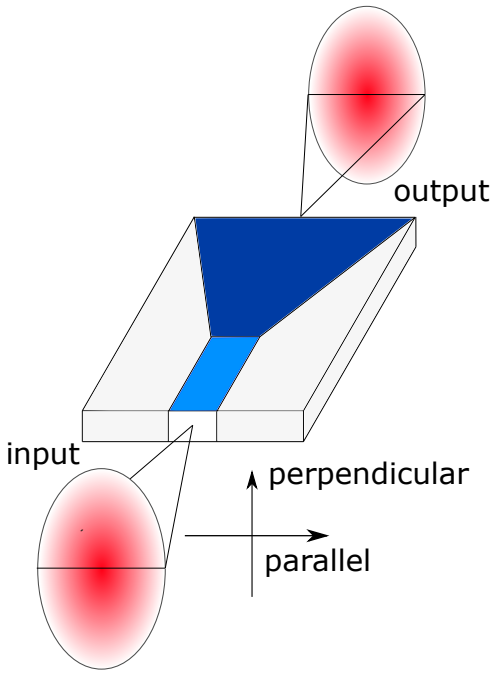

Figure 3.6.: Basic scheme of the input and output beams coming in and out of the tapered amplifier respectively. As it can be seen, the beam profile shape is elliptical due to the fact that the divergence perpendicular angle is greater than the horizontal one. Input: parallel angle 23°, perpendicular angle 40°. Output: parallel angle 18°, perpendicular angle 40°.

3.5. Fiber coupler

One of the main purposes of this work was to set up a modular amplifier system. The most convenient way to guide the seed beam and the output amplified beam was using optical fibers. However, the light coming out of a fiber is highly divergent as explained in *2.4 Optical fiber*. Therefore, a fiber coupler is needed in order to collimate the light coming out of the fiber and to couple the amplified beam into the output fiber. In the initial setup (V1), the PAF2-5B fiber coupler by Thorlabs [30] was used, that has a focal length of 4.6mm with the optical fiber PMC-780-5.1-NA012-3-APC-200-P by Schäfter + Kirchhoff GmbH. At first, this fiber coupler was used as the input and the output coupler in the setup because two PAF2-5B fiber couplers were available during the first weeks of the project. However, knowing the output divergence of the beam coming out of the TA in the perpendicular direction (40°) and the focal length of the aspherical lens AL2 used to collimate the beam coming out of the TA in the perpendicular direction (f=4.51mm), one can calculate that the beam width will be $w = 4.51tan(40/2) = 1.64mm$. Then, using (2.14), where the MFD of the optical fiber is used as ω_0, one can see that the ideal fiber coupler will have a focal length of about 15mm. However, still a power transmission efficiency of about 20% was

obtained through the output fiber coupler. In the upgraded version of the setup (V2), the output fiber coupler the PAF2P-15B model by Thorlabs [31] was used, which has a focal length of 15mm. The optical fiber P5-780PM-FC-2 by Thorlabs was used with this coupler. Using this configuration, V2, a coupling efficiency of about 50% was achieved. The total power transmission of each setup and also the coupling efficiency will be discussed in the results.

These fiber couplers allow to move the lens inside the lens in the X and Y direction, perpendicular to the direction of propagation, by only using one screw for each direction. It also allow to move the lens in the Z direction, the direction of propagation of the beam, but this time using 3 screws, which allows to tilt the lens in three different direction. These degrees of freedom of the fiber coupler make the coupling a lot easier, so using a fiber coupler with the same characteristics is highly recommended.

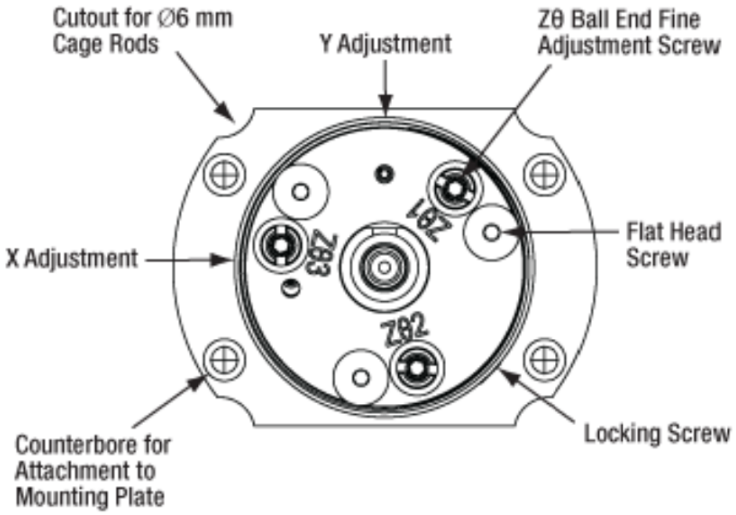

Figure 3.7.: Drawing of the fiber coupler PAF2-5B showing how to adjust the lens inside the coupler [30]. Here are shown the three screws to adjust the lens in the Z direction (direction of propagation), and also the position of the X and Y direction adjustment screws (perpendicular to the direction of propagation)

3.6. Optical isolator

To suppress the back reflected light coming into the TA output, an optical isolator was used, which functioning was explained in *2.3 Optical isolator*. This device was used because the TA is very sensitive to back reflected light coupling into the TA output, so it is very important to use an isolator in order not to damage the TA. In the setup, the 4mm aperture 780nm low power optical isolator provided by Electro-Optics Technology Inc. [32] was used.

About the power transmitted through the optical isolator, the manufacturer stated a transmission of >82%. However, around 80-85% power transmission efficiency was obtained through the optical isolator. The reason behind this lower than expected efficiency was that although the aperture of the optical isolator was bigger than the beam width, there was still some visible light from the beam that did not fit into the aperture of the isolator. Nevertheless, this loss is negligible if comparing our transmission with the one the manufacturer specifies.

3.7. Optical elements and setup alignment

About optical elements, in the designed setup 4 mirrors are necessary in order to guide the beam through the TA, CL and OI. Furthermore, two aspherical lenses are needed, one to guide the seed beam into the TA and another one to collimate the beam coming out of the TA in the perpendicular direction (See Fig.[3.6]). Finally, the use of a cylindrical lens is also necessary in order to collimate the amplified beam in the parallel direction before going through the optical isolator.

Figure 3.8.: TA mounted in with the two aspherical lenses calibrated at both sides. The visible red light coming out of the TA is the ASE output beam.

Two aspherical lenses (C230TMD-B 4.51mm Thorlabs)[33], one cylindrical lens (LJ1430L1-B Thorlabs)[34] and four mirrors were used (BK7 (dia12.7x3)mm HR > 99.5 @760-840, i45 EKSMA Optics)[35]. The 4.5mm focal length aspherical lenses were placed first at both sides of the TA mount. These lenses should be placed at its focal length distance from the TA, however, it is not possible to measure the distance between the lens and the TA with any physical measurement device because the TA is extremely sensitive. Therefore, the aspherical lenses were placed into the copper

mount and adjusted until achieving a collimated beam in the input as well as in the output of the TA. To do so, the rotary system provided by the mount of these lenses was used, where one could rotate the lens itself in the threaded mount to move it laterally on the direction of propagation.

To adjust these distances the TA was turned on at 600 mA and the seed laser of 780 nm at 5.1 mW, then a collimated beam in the perpendicular direction was achieved by collimating the beam to a reference point that was around 2m from the TA. Furthermore, images of the ASE input and output profile were taken in order to see if the lenses were correctly aligned (Fig.[3.9] and Fig.[3.10]). To do so, a powermeter (PM 100-A Thorlabs)[36], a sensor (S121C Thorlabs)[37] and a camera with a pixel size of 5.4μm (IDS UE-1540LE-M-GL with 30 dB attenuator)[38] were used. Also, to take the image of the beam, the beam profiler plugin of the software Micromanager was used.

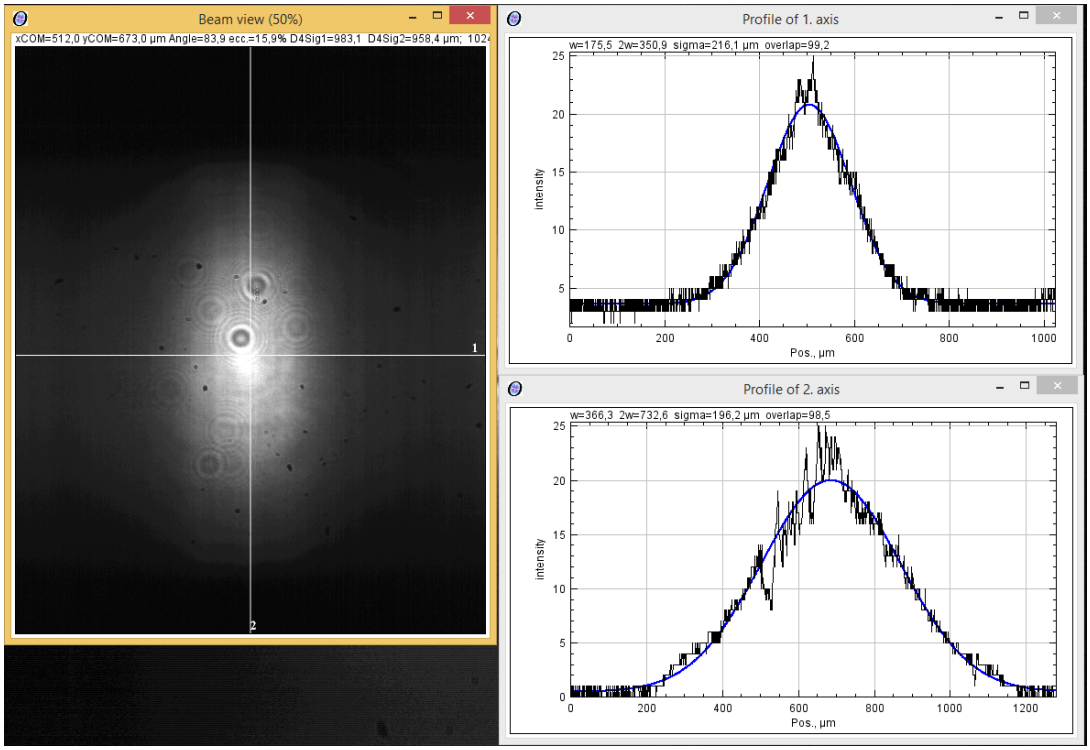

Figure 3.9.: ASE input beam profile of the tapered amplifier, with the input aspherical lens placed to obtain a colimated beam in the perpendicular direction ($\omega_x = 948\mu m$ and $\omega_y = 1978\mu m$).

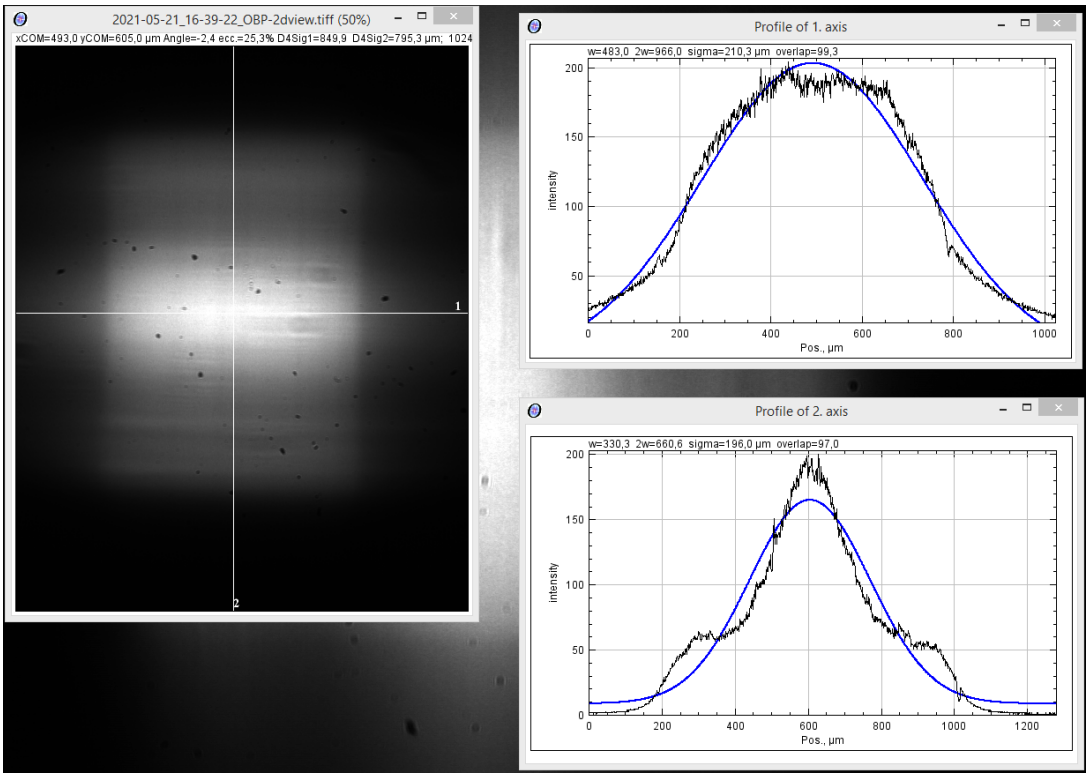

Figure 3.10.: ASE output beam profile after placing the output aspherical lens the same way as the input one.($\omega_x = 2608\mu m$ and $\omega_y = 1784\mu m$)

As it can be seen in Fig.[3.9], the ASE input beam profile has an elliptical shape, which is due to the fact that the beam has been collimated in the perpendicular direction as well has the shape of the TA as explained in *3.3 Tapered amplifier*. However, in the ASE output beam profile (Fig.[3.10]) a rectangular shape with three distinctive intensity peaks can be seen. This intensity profile in the Y direction ASE output profile is usual in tapered amplifier chips [24]. Nevertheless, later in this work it will be seen that the two external and smaller peaks will almost disappear when guiding the seed beam into the TA due to the superposition of the seed beam with the stimulated emission light of out the TA.
Once the aspherical lenses were placed in its optimal position, two mirrors (M1 and M2) were placed next to the input fiber coupler (FC1) as shown in Fig.[3.11] in order to be able to guide the seed beam into the TA.

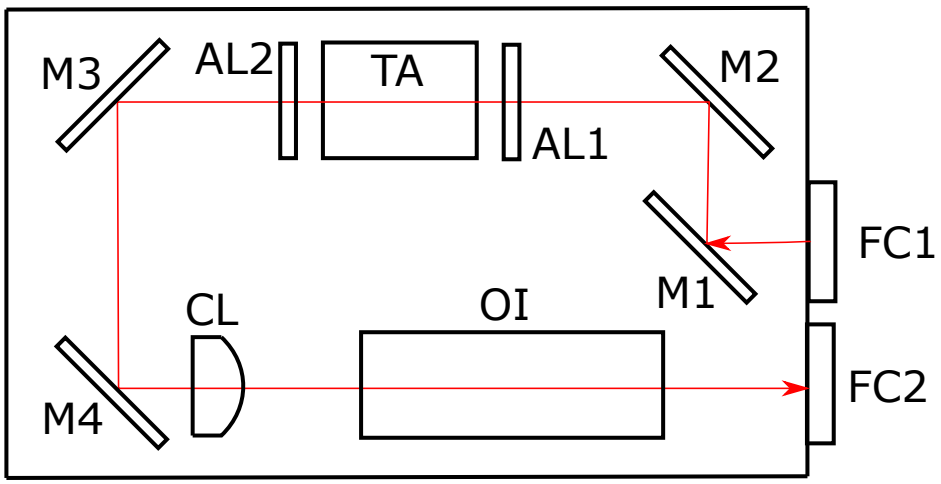

Figure 3.11.: Basic scheme of the final setup of the amplifier system. FC: Fiber coupler; M: Mirror; AL: Aspherical lens; TA: Tapered amplifier; CL: Cylindrical lens; OI: Optical isolator.

First, FC1 was calibrated as the manufacturer says in the manual [30]. The seed beam was guided through the FC1 using an optical fiber and using an alignment grid the beam was aligned in the X and Y direction (plane perpendicular to the direction of propagation). Then, the beam divergence was corrected in order to obtain a collimated beam. After that, M1 and M2 were placed in order to guide the beam into the TA as perfectly as possible, without any angle respect to the waveguide region of the TA. To do so, both mirrors were tilted vertically and horizontally. Finally, once the FC1 and the mirrors M1 and M2 were adjusted , a final adjustment was made using the powermeter PM 100-A [36] and the sensor S142C [40] to check the power out of the TA. Finely changing the configuration of the mirrors and the fiber coupler lens at the same time, the maximum output power for a certain input power and TA current was achieved. Specifically, an output power of $358mW$ was achieved for a seed power of $8.0mW$ and a TA current of $1.0A$. It is also important to consider the polarization of the seed beam, in the setup the polarization was adjusted in order to have the maximum output power. Polarization effect on the output power will be discussed in the results.

Once FC1, M1, M2, AL1 and AL2 were adjusted, an image of the output beam was taken in order to compare it with the ASE output profile. This image was taken at 100mm from AL2 using the camera IDS UE-154OLE-M-GL [38] with a 30dB attenuator plus another external 20dB atenuator. Furthermore, the polarization on the seed beam was also measured by the polarization analyzer SK010PA-700-1100nm by Schäfter+Kirchoff [39]. The seed beam was horizontally linear polarized with a minimum polarization extinction ratio (PER) = 21.1 dB. The minimum PER measures how much beam light is confined in a principal linear polarization mode, therefore, the higher Min. PER, the higher quantity of beam light is confined into the same

principal linear polarization mode.

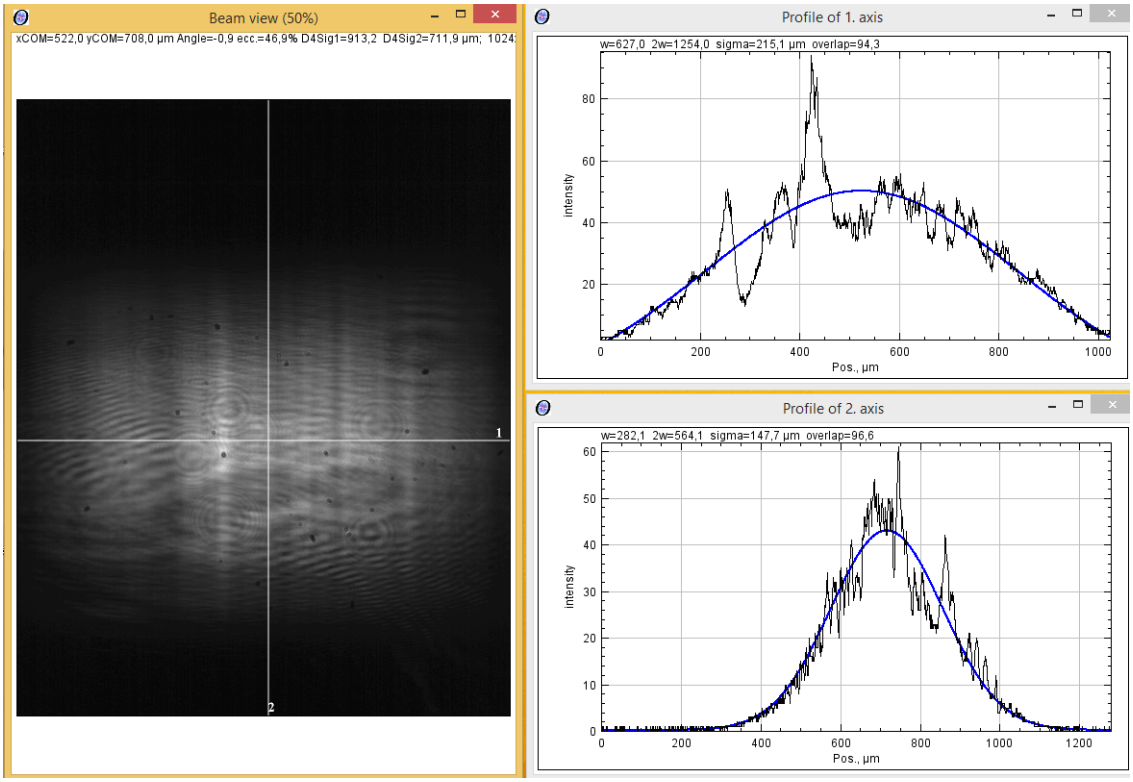

Figure 3.12.: Image of the output beam collimated in the perpendicular direction after AL2 at T=20.03ºC, input power = 9.5mW, output power = 29.4mW and TA current = 505mA, after passing trough two attenuators (20dB and 30dB). The beam width is $\omega_x = 3385\mu m$ and $\omega_y = 1523\mu m$

In Fig.[3.12] a clearly elliptical shape can be seen, because at this point the beam was only collimated in the perpendicular axis. The X/Y width ratio is about 2.22 at 100mm from AL2, so it was considered important to use a cylindrical lens in order to get a circular beam profile before the optical isolator. Whereas the beam diameter in the X direction was $2\omega_x = 6.77mm$ at 100mm, the aperture of the optical isolator which was at 115mm, was only 4mm. Therefore, it was necessary to use the CL before the OI in order to get as much light as possible through it.

Before placing the cylindrical lens, M3 and M4 were placed in the positions seen in Fig.[3.11]. After that, the cylindrical lens was placed just after M4. To do so, a custom mount was made for the cylindrical lens where one could move the lens perpendicular to the beam direction of propagation. The lens was glued into its custom made mount using UV curing adhesive. Regarding the election of making a custom made mount for the cylindrical lens and glue it with UV curing adhesive, that configuration was used because using a mount from the manufacturer would be

too big and it would have not allowed to place CL close enough to M4, where its ideal position is. Its ideal position was calculated knowing the focal length of the cylindrical lens in the X direction (f=59.99mm) and the divergence on the parallel axis of the output beam (18^{o}), where the aim was achieving a collimated beam with the same beam width in both axis. The focal length was selected to collimate the beam in the parallel direction and the position was chosen to match the beam width in the perpendicular direction.

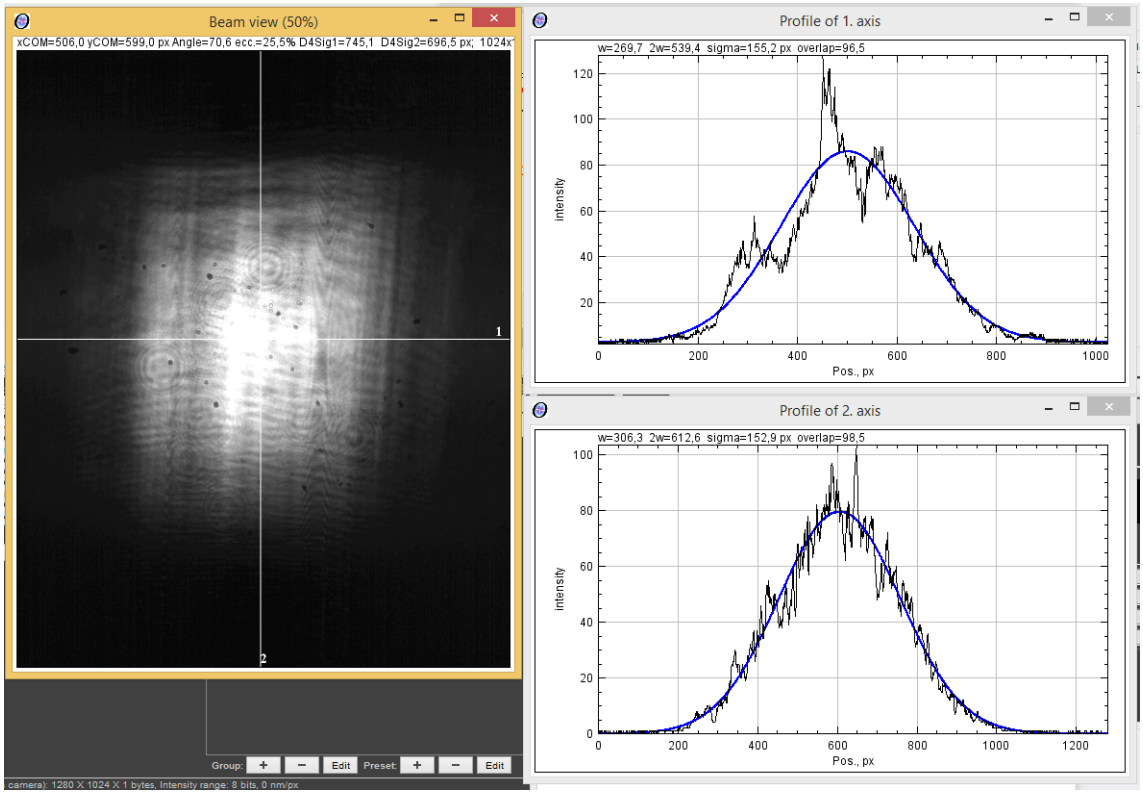

Figure 3.13.: Image of the beam profile after CL at T=20.03^{o}C, input power = 9.5mW, output power = 29.4mW and TA current = 505mA, after passing trough two attenuators (20dB and 30dB). The beam width is $\omega_x = 1456\mu m$ and $\omega_y = 1654\mu m$

After placing the cylindrical lens (CL), images of the beam profile were taken in order to see how circular the shape of the beam was. In this case, the same camera and configuration as in the image taken after AL2 were used, but now placing the camera after the cylindrical lens at 255mm from AL2. (See Fig.[3.13]). It is also very important to place the CL in the correct X axis position so the center of the beam crosses the CL at its center.

In this case a more circular alike shape than in Fig.[3.12] is seen. After the CL, a beam waist X/Y ratio of 0.88 was achieved. The beam width was then small enough to guide the beam into the optical isolator. After placing the isolator on the position seen in Fig.[3.11], M3 and M4 were adjusted in order to guide the beam as good as possible into the aperture of the isolator. To do so, both mirrors were placed at 45° and then tilted vertically and horizontally until aligning the centre of the beam with the center of the OI aperture. Then a sensor [37] was placed in the output of the isolator in order to see which configuration achieved the maximum output power.

As explained in *2.3 Optical isolator* a Faraday isolator was used, which is polarization dependent, so the isolator was rotated until getting the maximum output power. The direction of the linearly polarized output beam was matched with the direction of the input linear polarizer of the optical isolator.

Once this was aligned, mirrors M3 and M4 were finely tilted until getting the maximum output power. An output power of 22.3 mW was achieved for an input power = 9.5 mW, T = 20.03 °C and TA current = 505 mA. Directly comparing this output power result with the one we measured after AL2, a loss of power of about 25% was seen from AL2 to after OI. However, this loss of power decreased by 10-15% in the final calibration once everything was mounted and adjusted. Apart from that, an image of the beam profile out of the optical isolator was taken in order to compare it with the beam profile just after the CL.

In Fig.[3.14] it can be seen that the beam profile is more circular than it was before the OI. However, it can also be seen here that the beam width in the Y axis decreased after passing through the isolator. Even though the beam width before the isolator (See Fig.[3.13]) was smaller than the aperture of the isolator (d=4mm), some light on the Y border of the beam was lost due to reflections near the aperture. However, the power loss experienced due to those reflections was only of about 2-5% as stated in *3.6 Optical isolator*.

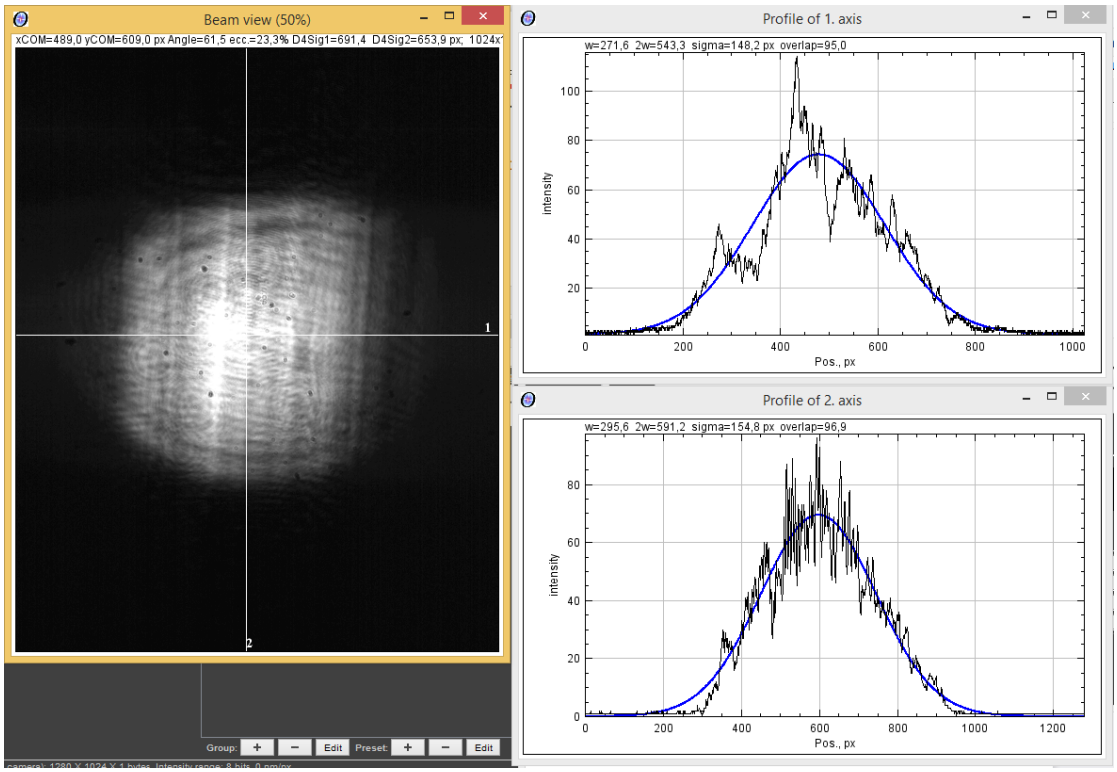

Figure 3.14.: Image of the beam profile after the OI at T=20.03ºC, input power = 9.5mW, output power = 22.3mW and TA current = 505mA, after passing trough two attenuators (20dB and 30dB). The beam width is $\omega_x = 1467\mu m$ and $\omega_y = 1596\mu m$

Finally, another adjustment of the FC2 and also M3 and M4 was needed again in order to obtain the maximum power out of the output fiber. To adjust the FC2, the adjustment process done on FC1 was first followed. Guiding the seed beam through the fiber, the outcoming beam was aligned in the X and Y direction (plane perpendicular to direction of propagation) and also was collimated. However, in this case the adjustment was not as good as in FC1 because as calculated in *3.6 Fiber coupler* a 15mm fiber port was needed instead of a 4.6mm one. Therefore, when shooting the beam coming out of the optical isolator into FC2, to adjust it was needed in order to obtain the maximum power, but still some power was lost because shooting the beam into the fiber at beam width equal to the MFD of the fiber is not possible in this case. Also it is important to consider the loss due to the fact that the beam coming out of the OI was not perfectly gaussian (See Fig.[3.14]). Finally, once the FC2 was adjusted, after the output fiber it was obtained an output power of 5.1mW for a seed power = 9.5 mW, T = 20.03 °C and TA current = 505 mA. Using the same configuration, 22.3mW of optical power where measured after the OI and 29.4mW after FC1. Finally, the same output coupler adjustment process was followed in order to place the 15mm fiber coupler into the setup.

4. Results

In this chapter, the measurements taken for the described setup are compared with the results presented in the Jayampathi C. B. Kangara et al. paper [8]. In this paper, a similar setup configuration was used, therefore, it was decided to take the same measurements in order to be able to compare the setup described in this thesis with the one described in the paper. The measurements taken were: seed power vs. output power, TA current vs. output power and input beam polarization angle vs. output power. First, the measurements taken using the free beam (FB) configuration (See Fig.4.1) are presented. Then, the results obtained using the version V1 are discussed, using fiber couplers with the same coupling lens focal distance in the input and the output. Finally, the measurements taken on the improved version of the setup, V2, are explained, using a fiber coupler with a coupling lens focal distance of 15mm as the output fiber coupler, FC2.
Regarding the errors, for the polarization angle and the current measurements, the display accuracy was considered and in the power measurement, the error given by the manufacturer was considered because it is bigger than the fluctuations seen while taking these measurements. For the output and input power measurement an error of $\pm 3\%$ [36] was considered, for the polarization angle the error was $\pm 1^{\circ}$ and for the TA current an error of 0.1mA. Finally, it was decided not to show the errors in the respective graphs as they were not comfortably visible.

4.1. Free beam configuration results

Regarding the results of the free beam configuration, the obtained results were directly compared with the ones in [8] as a similar configuration was used. Measurements using a free beam configuration were taken to evaluate the behaviour of the collimated beam out of the TA before mounting the whole system, especially the output power achieved.

To measure the output power, the power sensor S142C [40] and the powermeter PM 100-A [36] were used. Furthermore, a half-wave plate and two external mirrors to guide the beam into the TA were used. To adjust the mirrors the same steps as the steps explained in *3.7 Optical elements and setup alignment* were followed. In this setup an optical isolator was not used because the power sensor integrates an Ulbritch sphere, which does not have any reflective surface. Therefore, there is no risk of damaging the TA.

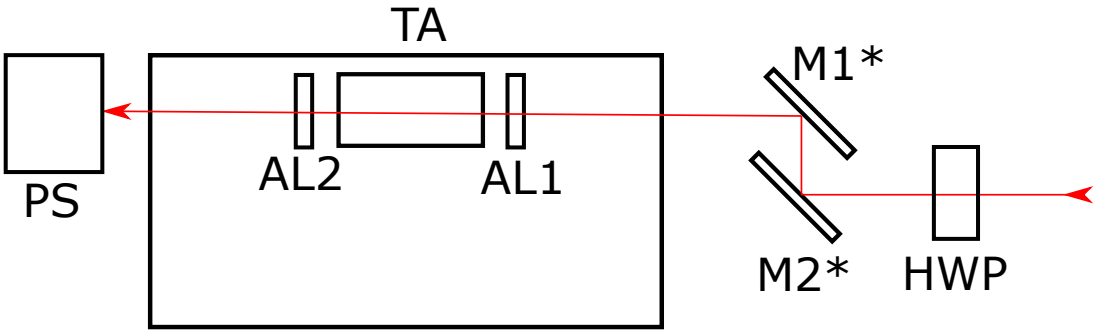

Figure 4.1.: Basic scheme of the free beam configuration used in order check the behaviour of collimated beam coming out of the TA. No optical isolator was used in this setup, since the S142C [40] power sensor uses an Ulbricht sphere, which does not feature reflective surfaces. M1* and M2* are not the same mirrors used in the final setup, HWP: half-wave plate, PS: Power sensor; AL: Aspherical lens, TA: Tapered amplifier

In Fig.[4.2(a)] a maximum amplification of 25.6 dB is seen, apart from the fact that the amplification was reduced when using more seed power. This data is directly extracted from the one in Fig.[4.2(b)]. In the latter, the curve gets flat when increasing the input power. This happens when, for a constant TA current (constant number of electrons that can decay by stimulated emission), there are so many seed photons that the probability of stimulating a photon emission is significantly reduced. In Fig.[4.2(c)], the output power in dependency on the TA current is shown. At lower TA currents the behaviour is not linear. The reason behind this behaviour is that the population inversion is not effective enough at these currents with the seed power used. A simplified explanation of this is effect is found in *2.2 Optical amplification in a semiconductor gain medium.* In Fig.[4.2(d)], the polarization dependency of the TA output beam power is shown. The system is very sensitive to polarization changes, whereas at 0° the output power is 800 mW, at 90° is only around 200 mW. The TA used in this setup produces the maximum amplification power when the seed photon E field is perpendicular to the junction plane of the TA, TM mode.[29].

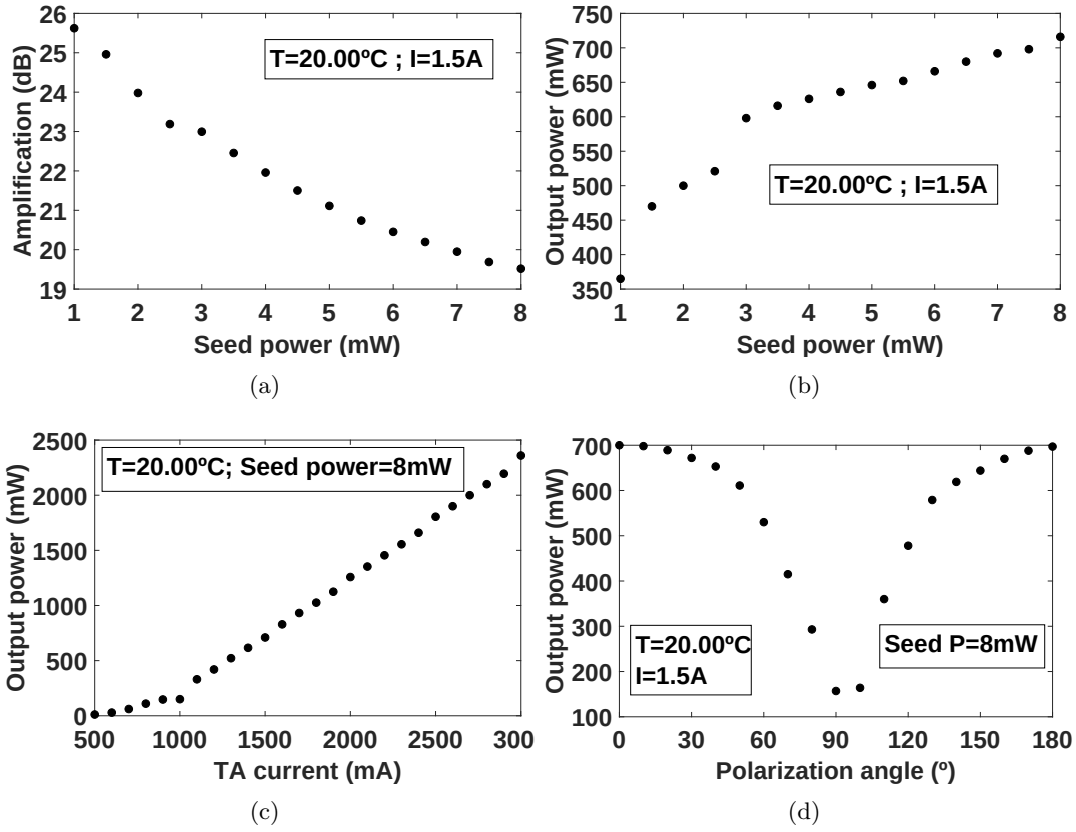

Figure 4.2.: Graphs of the free beam configuration. (a) Amplification achieved depending on the input power, using constant temperature and current. (b) Results of input versus output power, with both constant temperature and TA current. (c) Output power generated by the TA using different currents, keeping constant the seed beam power and temperature. (d) This figure shows the dependency of the TA output power with the seed beam polarization angle.

4.2. V1 configuration results

Regarding the results of the V1 configuration setup, the same measurements as in the free beam configuration were taken, except the polarization dependency. The optical isolator input polarizer was aligned to the seed beam polarization, producing the most output power after the isolator, so there were no expected changes in polarization dependency compared with the free beam configuration. In the V1 setup configuration the measurements were taken in three different points: after AL2, after OI and after the output optical fiber (See Fig.[3.11]). The data measured after AL2 is represented by '•', the measurements after OI by '○' and the data measured coupled into the output fiber by '▲'.

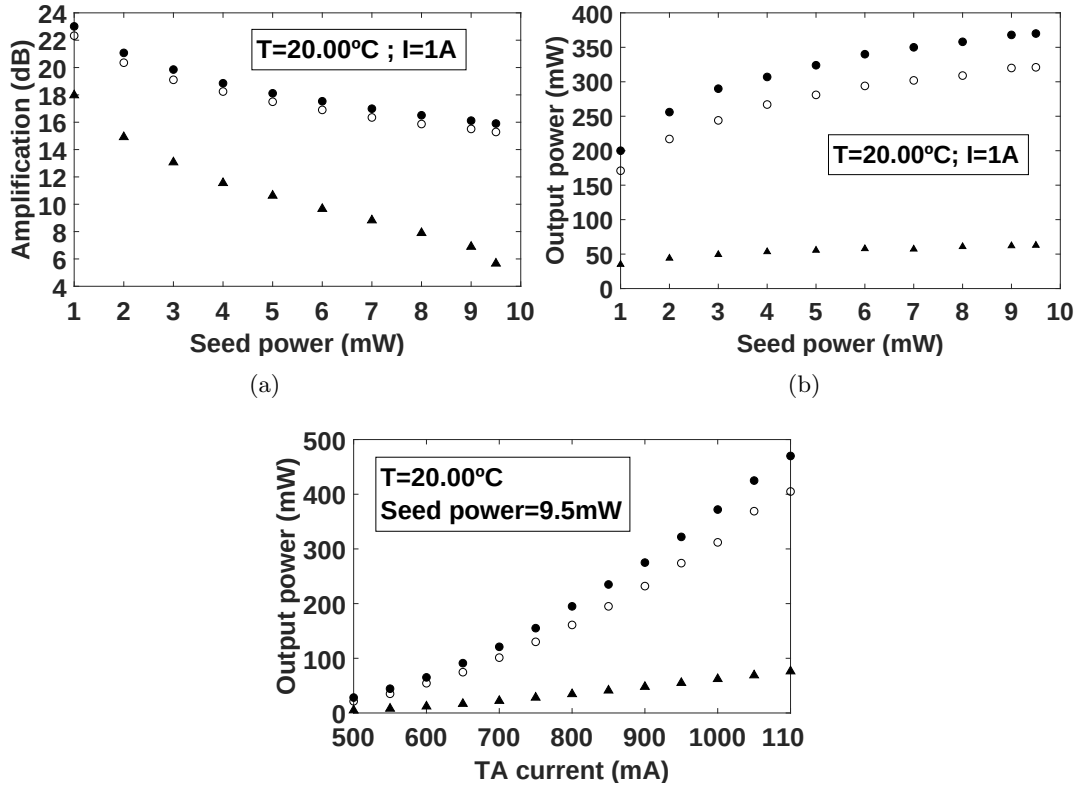

Figure 4.3.: Graphs of the V1 configuration. (a) Amplification achieved depending on the input power, using constant temperature and current, at three different points in the setup (● = after AL2, ○ = after OI, ▲ = after output fiber). (b) Results of input versus output power at those same points, with both constant temperature and TA current. (c) Output power generated by the TA using different currents at the same three different points, here using constant input power and temperature.

In Fig.[4.3(a)] the main loss of power is due to the coupling of the amplified beam into the output fiber. The average transmission efficiency through the optical isolator is around 85%, and around 20% coupling efficiency in the FC2. The mean power transmission efficiency through the setup was 18%. Regarding the amplification on each stage of the setup a maximum of 23.0 dB is seen just after AL2 and 15.4 dB after the output fiber. Directly comparing this results with the ones in [8], the measured amplification after the optical isolator in the V1 setup is significantly bigger than theirs after the CL using 2/3 of the TA current they used (both experiments runned at the same temperature). About Fig.[4.3(c)] the output power increases, at every measured point, almost linearly when increasing TA current at constant seed beam

power. However, the linear approximation works worse here than in Fig.[4.2(c)]. In Fig.[4.3(c)], also a quadratic behaviour is seen at lower TA current.
In conclusion, the mean coupling efficiency is 21% while the mean power transmission across the whole setup is 18%, which is not enough to couple more than 100mW in the output fiber, one o the main requirements the TA system was designed for.

Finally, apart from the data extracted from the measurements, is also important to remark some behaviours seen while setting up the system and taking measurements. For example, the system was stable while taking measurements, but it was not when adjusting the output fiber coupler lens. In general, the coupling efficiency is measured comparing the optical power before the coupling and after the fiber, where one would get a coupling efficiency dependency with the position of the fiber coupler lens in the direction of propagation. In the V1 setup, this coupling efficiency vs position of the lens presented a narrow maximum peak, therefore when slightly adjusting the output fiber coupler lens from the most optimal position, the output power would drastically decrease. This happened because a 4.6mm fiber port was used instead of a 15mm one, which would be more suitable as explained in *3.5 Fiber coupler*. The other devices did not reproduce the same problems as the fiber couplers.

4.3. V2 configuration results

About the results of the V2 configuration setup, the same measurements as in the previous section were taken. However, in the seed power vs output power measurements, it was not possible to measure the output power after AL2. Once the setup was mounted, it was not possible measure the power after AL2 with the sensor S142C [40], as done before in the V1 setup, where the box back plate was not mounted, because it was not possible to bring it close enough to the beam or even into the housing of the setup. Therefore, the sensor S121C [37] had to be used, for which back reflections into the TA were observed while measuring the beam power. For security reasons it was decided not to measure the output power in that position. Regarding the graphs in Fig.[4.4],the data measured after AL2 is represented by '•', the measurements after the OI by '○' and the power measured coupled into the output fiber by '▲'.

Directly comparing these results with the ones in the previous section, less power loss across the whole system is seen. For example, if comparing Fig.[4.4(a)] with Fig.[4.3(a)] it can be seen that the maximum amplification was 1.5dB larger in the V2 configuration. Also, in the V2 configuration more than 100mW of output power were achieved inside the output fiber (See Fig.[4.4](a)), which was the main motivation of building this amplifier. This can also be seen in Fig.[4.4(c)], where more than 100mW of output power was achieved when using more than 800mA TA current at $T = 20.00°C$ and 9.5mW of seed beam power.

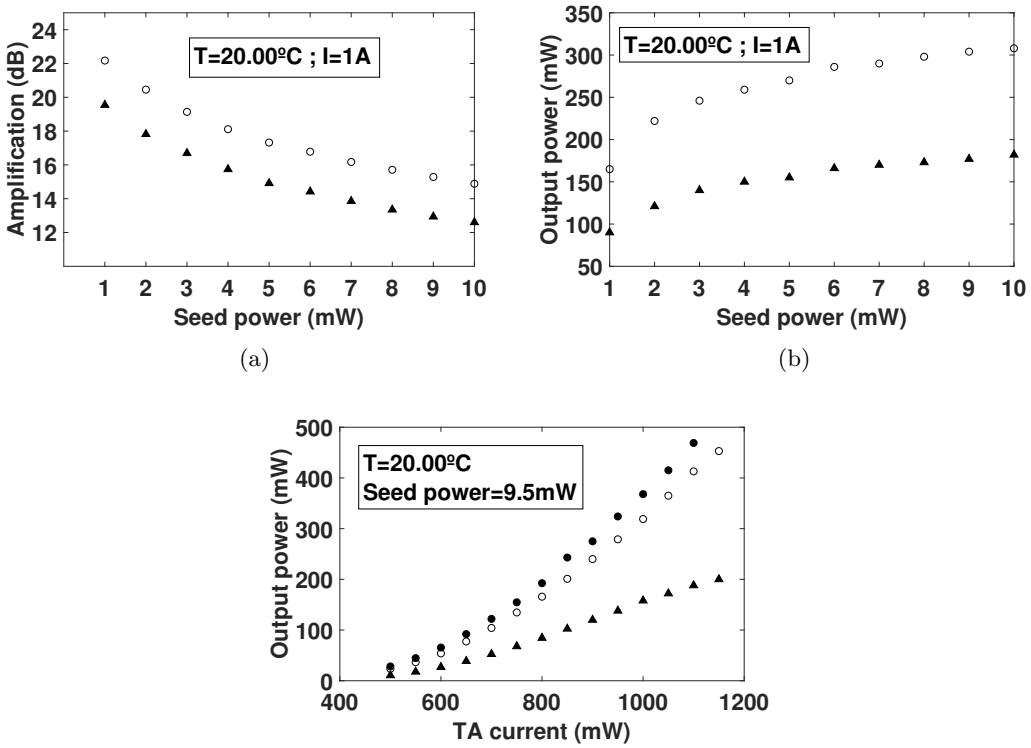

Figure 4.4.: Graphs of the V2 configuration. (a) Amplification achieved depending on the input power, using constant temperature and current, at two different points in the setup (∘ = after OI, ▲ = after output fiber). In this case no measurement was taken after AL2 for security reasons, further explanation is given in the text below. (b) Results of input versus output power at those same points, with both constant temperature and TA current. (c) Output power generated by the TA using different currents at the same three different points as in the V1 configuration (• = after AL2), here using constant input power and temperature.

Using this configuration a mean, coupling efficiency of 53% and a mean power transmission of 42% across the whole setup were achieved. Therefore, using the 15mm fiber coupler increased the mean power transmission of the setup by 24% and the coupling efficiency by 32% resulting in more than a doubled overall power transmission, as well as coupling efficiency. Furthermore, the maximum coupling efficiency measured was 59%, which is significantly larger than the one measured in published papers that use a similar configuration[8][41]. Regarding the output power achieved after the output optical fiber, the measured maximum 200mW was achieved only using one fourth of the possible current the TA can be used with. Therefore, higher output optical powers can be achieved in this system. Measurements of those

higher power regimes were not taken due to the optical power limit of the available power sensors and to not damage the output optical fiber.

To measure the stability, the system was moved horizontally and vertically with both hands. Losses of about 10% were seen while slowly moving the system, however, these losses were corrected automatically when the movement stopped. When the system was moved more aggressively, the losses were about the same magnitude but were not automatically corrected upon stopping the motion. Nevertheless, it was possible to adjust the system again in a few minutes. Finally, hits were delivered on the lateral plates of the box and losses of about 95% were seen. In this case it was also possible to reproduce the initial output power after a couple of minutes of readjustment.

5. Conclusion

The main purpose of this project was building a stable miniaturized laser amplifier system that could deliver output optical powers of at least 100mW. In this chapter, the building process that was followed and the results of the built setup are analyzed, comparing them with the original design and expected results, respectively. Finally, it will be explained how the setup can be improved for better results in the future.

Comparing the initial design with the V2 one (Fig.[3.11]), only one modification was done, the initial output fiber coupler was replaced by the optimal one. After adjusting the output aspherical lens AL2, one could already calculate that the ideal output fiber coupler would be a 15mm focal length one, as it was shown in *3.5 Fiber coupler*. Therefore, replacing the original FC2 was necessary. Furthermore, after placing the 15mm focal length FC2 in the setup, not only more optical output power was achieved, but also the adjusting time was reduced. Regarding the custom made mount for the cylindrical lens, it fitted into the setup without the need of rebuilding the original aluminium box. Finally, in the aluminum box there was space for a waveplate. Although it was not introduced in the setup, it is necessary to include a waveplate to control the polarization of the beam coming out of the output fiber. In the taken measurements only the power was measured, therefore, the inclusion of a waveplate would not have any effect on the presented measurements.

As to the portability, the setup is small enough to be carried using only one hand, specific measurements can be found in the Appendix C. When it comes to the stability of the setup, the system was hit and moved horizontally and vertically. The setup was stable against movements but not to lateral soft hits. The reason behind this is that the setup box is made of six plates which makes it less resilient when it comes to lateral hits. This problem could be solved by cutting the box out of one block and only using one attachable wall for adjustment reasons.

Regarding the results, the initial free beam configuration measurements were quite promising compared to the Jayampathi C. B. Kangara et al. paper [8], where they used a similar setup. The results from the V1 configuration, however, were not as good as desired, where the optical powers coupled into the fiber did not achieve the objective of having minimum 100mW output power measured after the output fiber at any measurement taken. Nevertheless, as it can be seen in the section *4.3 V2 configuration results*, a mean coupling efficiency of 53% was achieved under the V2 configuration, with a maximum of 60% coupling efficiency. This coupling is actually comparable to general free space coupling efficiencies of diode lasers. Moreover,

this coupling efficiency was larger than the efficiency presented in published paper measurements that used a similar configuration [8][41]. The measured output powers also fulfill the power requirement stated in the introduction. Therefore, the built setup can be used to test space experiment setups.

In conclusion, only one element was changed in order to improve the setup, which did not had an impact in the box design. Furthermore, there is space to place a waveplate to control the polarization of the beam coming out of the fiber. However, to solve stability problems, the box itself should be redesigned in order to be resilient against lateral hits. Apart from that, the setup achieved the desired power coupled into the output fiber, 100mW, obtaining a maximum coupling efficiency superior to published papers that used a similar setup.

References

[1] Belew, Leland F.; Stuhlinger, Ernst.Research programs on Skylab. SKYLAB: A Guidebook NASA. p. 114. Retrieved July 10, 2020

[2] Yannick Bidel, Olivier Carraz, Renée Charrière, Malo Cadoret, Nassim Zahzam, and Alexandre Bresson. Compact cold atom gravimeter for field applications. Appl. Phys. Lett. 102, 144107 (2013) https://doi.org/10.1063/1.4801756

[3] S. Riedl, G. W. Hoth, B. Pelle, J. Kitching and E. A. Donley. Compact atom-interferometer gyroscope based on an expanding ball of atoms. 2016 J. Phys.: Conf. Ser. 723 012058.

[4] Soriano, M., Aveline, D., Mckee, M., Virkler, K., Yamamoto, C., and Sengupta, A. (2014). Cold atom laboratory mission system design. 2014 IEEE Aerospace Conference. doi:10.1109/aero.2014.6836202

[5] Moritz Mihm, Jean Pierre Marburger, André Wenzlawski, Ortwin Hellmig, Oliver Anton, Klaus Döringshoff, Markus Krutzik, Achim Peters, Patrick Windpassinger, the MAIUS Team. ZERODUR® based optical systems for quantum gas experiments in space. Acta Astronautica, Volume 159, 2019. ISSN 0094-5765. https://doi.org/10.1016/j.actaastro.2019.03.060.

[6] J. P. Marburger, Moritz Mihm, Ortwin Hellmig, André Wenzlawski, Patrick Windpassinger.Highly stable Zerodur based optical benches for microgravity applications and other adverse environments. Proc. SPIE 11180, International Conference on Space Optics — ICSO 2018, 1118052 (12 July 2019). https://doi.org/10.1117/12.2536101

[7] Toptica Photonics. Amplified Lasers. High-power diode lasers and amplifiers. https://www.toptica.com/products/tunable-diode-lasers/amplified-lasers/

[8] Jayampathi C. B. Kangara et al. Design and construction of cost-effective tapered amplifier systems for laser cooling and trapping experiments. Am. J. Phys. 82 (8), August 2014. http://dx.doi.org/10.1119/1.4867376

[9] Amarasinghe, D., Ruseckas, Arvydas , Vasdekis, Andreas , Goossens, Mark , Turnbull, Graham , Samuel, Ifor. 2006. Broadband solid state optical amplifier based on a semiconducting polymer. Applied Physics Letters. 89.

[10] Alabbas A. Al-Azzawi, Aya A. Almukhtar, P.H. Reddy, D. Dutta, S. Das, A. Dhar, M.C. Paul, U.N. Zakaria, H. Ahmad, S.W. Harun, Compact and flat-gain fiber optical amplifier with Hafnia-Bismuth-Erbium co-doped fiber,Optik,Volume

References

170,2018,Pages 56-60,ISSN 0030-4026, https://doi.org/10.1016/j.ijleo.2018.05.104

[11] Eagleyard Photonics. Data sheet. EYP-TPA-0780-02000-4006-CMT04-0000 Revision 1.06.

[12] Baxter, Rodney J. (1982). Exactly solved models in statistical mechanics. Academic Press Inc. ISBN 9780120831807.

[13] Anthony E. Siegman Lasers. Chapter 6 University Science Books, 1986

[14] Mayavanshi, Manisha and Prajapati, Dr. Pravin and Gharge, Anuradha. (2011). Simulation of Polarization Dependent Gain in Semiconductor Optical Amplifier. 10.13140/2.1.2053.4085.

[15] Schäfter + Kirchhoff GmbH. Data sheet. PMC-780-3-18-200

[16] R. Rosenberg, C. B. Rubinstein, and D. R. Herriott, Resonant Optical Faraday Rotator Appl. Opt. 3, 1079-1083 (1964).https://www.osapublishing.org/ao/abstract.cfm?URI=ao-3-9-1079

[17] Vojna, David; Slezák, Ondřej; Lucianetti, Antonio; Mocek, Tomáš (2019). Verdet Constant of Magneto-Active Materials Developed for High-Power Faraday Devices. Applied Sciences. 9 (15): 3160. doi:10.3390/app9153160.

[18] The Fiber Optic Association Inc. The FOA Reference For Fiber Optics - Optical Fiber April 10, 2016. www.thefoa.org

[19] Guenther, Robert D. Modern Optics / Robert D. Guenther. Duke University, 1990. ISBN-0-471-60538-7

[20] Michael R. Vastag Mode Field Diameter and Effective Area October, 2001.

[21] Andrew M. Kowalevicz, Jr., Frank Bucholtz. Beam Divergence from an SMF-28 Optical Fiber(NRL/MR/5650–06-8996) Naval Research Laboratory, Washington, DC, 2006.

[22] Anthony E. Siegman Lasers. Chapter 17 University Science Books, 1986

[23] Sören Boles. QOQI member at JGU. https://www.qoqi.physik.uni-mainz.de/team/soeren-boles/

[24] Albrodt , P., Jamal, M. T., Hansen, A. K., Jensen, O. B., Niemeyer, . M., Blume, G., ... Lucas-Leclin, G. (2019). Recent progress in brightness scaling by coherent beam combining of tapered amplifiers for efficient high power frequency doubling. In Proceedings of SPIE (Vol. 10900). [109000O] SPIE - International Society for Optical Engineering. Proceedings of SPIE, the International Society for Optical Engineering, Vol.. 10900, DOI: 10.1117/12.2508443

[25] Toptica Photonics. Tunable diode laser available with digital control DLC pro https://www.toptica.com/products/tunable-diode-lasers/ecdl-dfb-lasers/dl-pro/

[26] Marlow Industries RC3-6-01LS https://www.digikey.de/product-detail/de/marlow-industries-inc/RC3-6-01LS/1681-1061-ND/6159109

References

[27] ILX Lightwave LDC-3744c https://www.newport.com/p/LDC-3744C-220V

[28] Numista. 1 Euro Cent https://en.numista.com/catalogue/pieces105.html

[29] Eagleyard Photonics. 780nm 2W C-mount tapered amplifier https://www.toptica-eagleyard.com/products/tapered-amplifiers/tapered-amplifiers-780nm-2000-mw/

[30] Thorlabs. PAF2-5B - FiberPort. https://www.thorlabs.com/thorproduct.cfm?partnumber=PAF2-5B

[31] Thorlabs. PAF2P-15B - FiberPort. https://www.thorlabs.de/thorproduct.cfm?partnumber=PAF2P-15B

[32] Electro-Optics Technology Inc. Tornos Low Power Optical Isolators https://www.eotech.com/cart/131/faraday-rotators-and-isolators/tornos-faraday-rotators-and-isolators---500-nm-to-1064-nm/tornos-low-power-optical-isolators---500-nm-to-1030-nm

[33] Thorlabs. C230TME-B - Aspherical Lens https://www.thorlabs.com/thorProduct.cfm?partnumber=C230TME-B

[34] Thorlabs. LJ1430L1-B - Cylindrical Lens https://www.thorlabs.de/thorProduct.cfm?partNumber=LJ1430L1-B

[35] ESKMA Optics. BK7 Mirrors https://eksmaoptics.com/optical-components/dielectric-mirrors/bk7-laser-line-mirrors/

[36] Thorlabs. PM100A - Compact Power Meter Console. https://www.thorlabs.de/thorProduct.cfm?partNumber=PM100A

[37] Thorlabs. S121C - Standard Photodiode Power Sensor. https://www.thorlabs.com/thorproduct.cfm?partnumber=S121C

[38] IDS Imaging Development Systems GmbH. UI-1540LE-M-GL. https://www.gophotonics.com/products/scientific-industrial-cameras/ids-imaging-development-systems-gmbh/45-641-ui-1540le-m-gl

[39] Schäfter + Kirchhoff GmbH. Polarization Analyzer SK010PA https://www.sukhamburg.com/products/fiberoptics/measurement/polarizationanalyzer.html

[40] Thorlabs. S142C - Integrating Sphere Photodiode Power Sensor. https://www.thorlabs.com/thorproduct.cfm?partnumber=S142C

[41] Xiong, Y. (2006). Design and characteristics of a tapered amplifier diode system by seeding with continuous-wave and mode-locked external cavity diode laser. Optical Engineering, 45(12), 124205. doi:10.1117/1.2404925

A. Acknowledgements

It would have been impossible for me to finish this thesis on my own. Therefore, I would like to thank everyone who has supported me for their contributions.

First of all, I would like to thank Dr. Patrick Windpassinger for giving me the oppourtinity to write this thesis in his group, the QOQI group at the JGU. I am also very thankful for his friendly and warm treatement and for making me feel included in the group. I also want to thank Dr. Klaus Wendt for kindly agreeing to be the second examiner in such short notice.
Specially, I would like to thank Sören Boles, my supervisor, who helped me a lot while building the setup in the lab and also who corrected this thesis a lot of times. Here I also want thank André Wenzlawski for reading this thesis and for the very useful comments. I could not have had such a great time doing this thesis if it wasn't for Parvez Islam, Ishan Varma and also Sören Boles, who made me feel at home in the office and at lunch time.

I would like to thank my family for the uncondinitional support over the years and for making it possible for me to study what I always wanted. I would also like to include my closest friends here, who made it a lot easier for me to write this thesis and who have always supported me.

Finally, I would like to thank the University of Valencia for giving me the opportunity to do an Erasmus semester in Mainz.

B. List of the components used

Device	Model	Manufacturer
ECDL	DL_pro_018064	Toptica Photonics
Controller	LDC-3744C	ILX Lightwave
Peltier element	RC3-6	Marlow Industries Inc.
Tapered amplifier	780nm 2W C-mount	Eagleyard Photonics
Aspherical lens	C230TMD-B 4.51mm	Thorlabs
Mirror	BK7 dia(12.7x3)mm HR>99.5% 760-840, i45	EKSMA Optics
Powermeter	PM 100-A	Thorlabs
Power sensor	S121C	Thorlabs
Camera	UE-154OLE-M-GL	IDS
Polarization analyzer	SK010PA-700-1100nm	Schafter+Kirchoff
Power sensor	S142C 350-1100nm Pmax 5W	Thorlabs
Optical fiber FB conf.	60FC-4-A7.5-02	Schafter+Kirchoff
Optical fiber V1	PMC-780-5.1-NA021-3-APC-200-P	Schafter+Kirchoff
Fiber coupler V1	PAF2-5B	Thorlabs
Output fiber coupler V2	PAF2P-15B	Thorlabs
Output optical fiber V2	P5-780PM-FC-2	Thorlabs
Optical isolator	TORNOS Low Power Optical Isolator - 780nm	Electro Optics Technology Inc.

C. Custom made designs/drawings

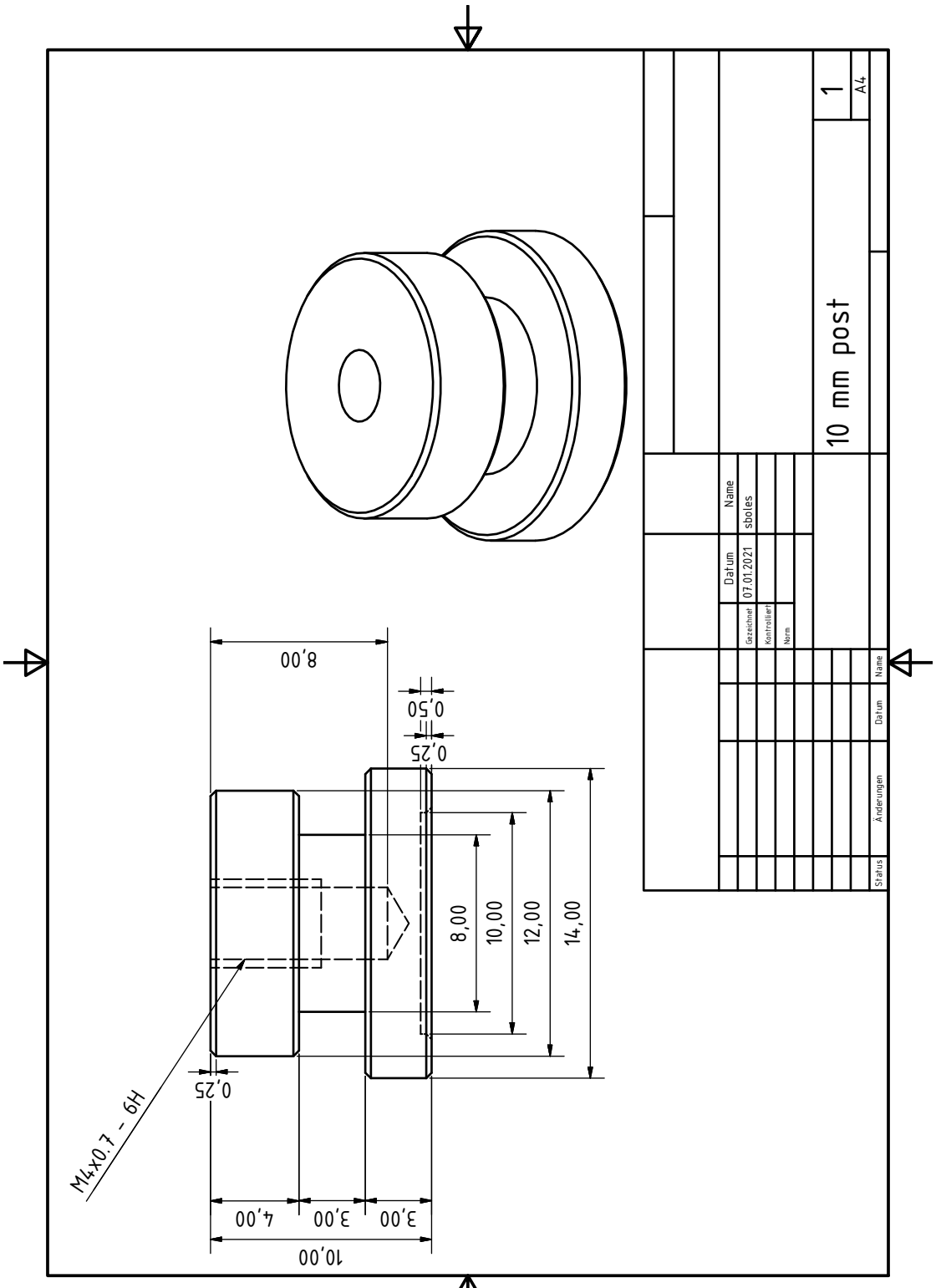

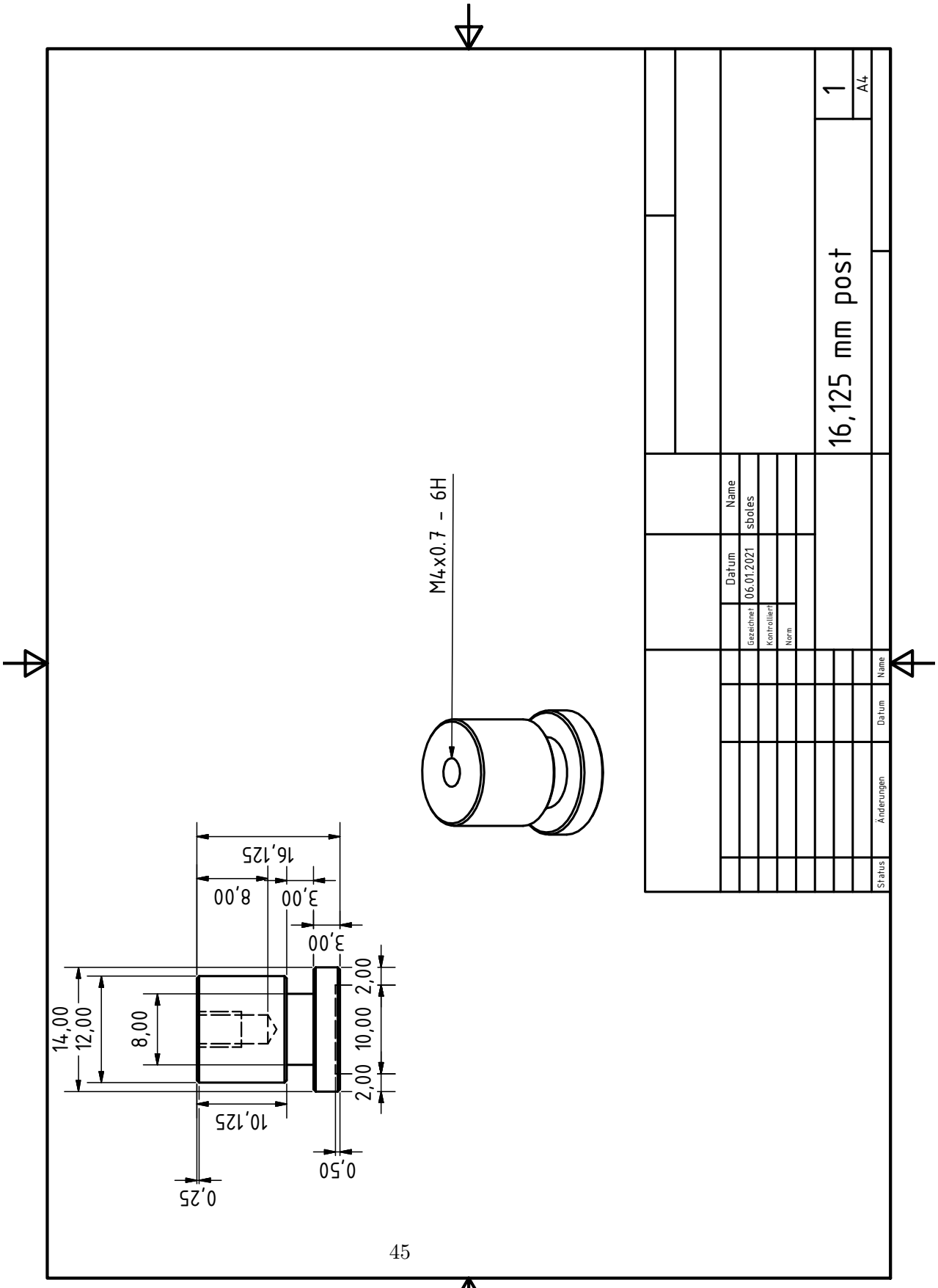
16,125 mm post
1
A4
Name
sboles
Datum
06.01.2021
Gezeichnet
Kontrolliert
Norm
Name
Datum
Änderungen
Status
M4x0.7 - 6H
16,125
8,00
3,00
3,00
2,00
10,00
2,00
14,00
12,00
8,00
10,125
0,50
0,25

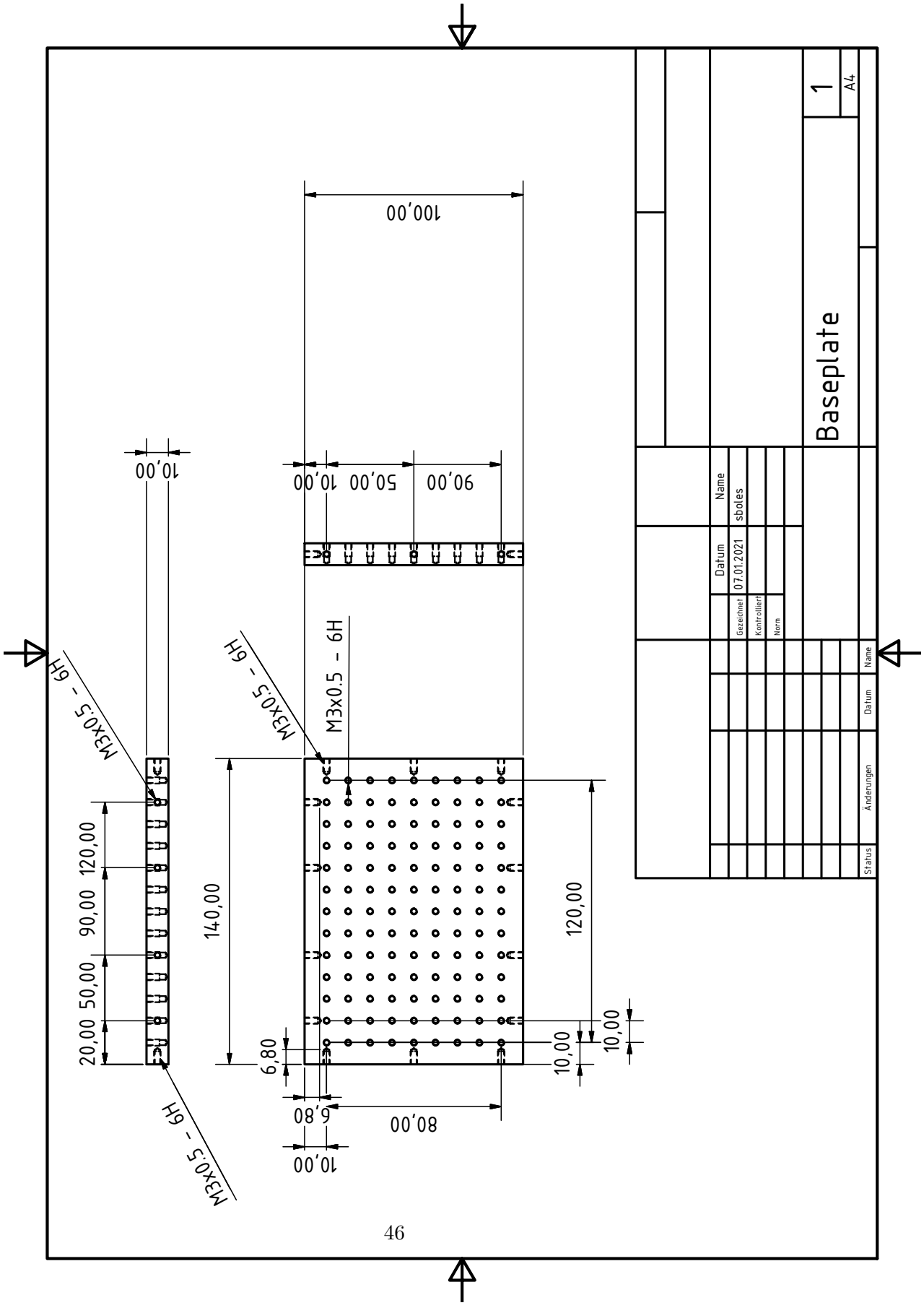
Baseplate
1
A4
Name
sboles
Datum
07.01.2021
Gezeichnet
Kontrolliert
Norm
Status
Änderungen
Datum
Name
100,00
10,00
50,00
90,00
10,00
M3x0.5 - 6H
M3x0.5 - 6H
M3x0.5 - 6H
140,00
120,00
120,00
90,00
50,00
20,00
6,80
6,80
80,00
10,00
10,00
10,00

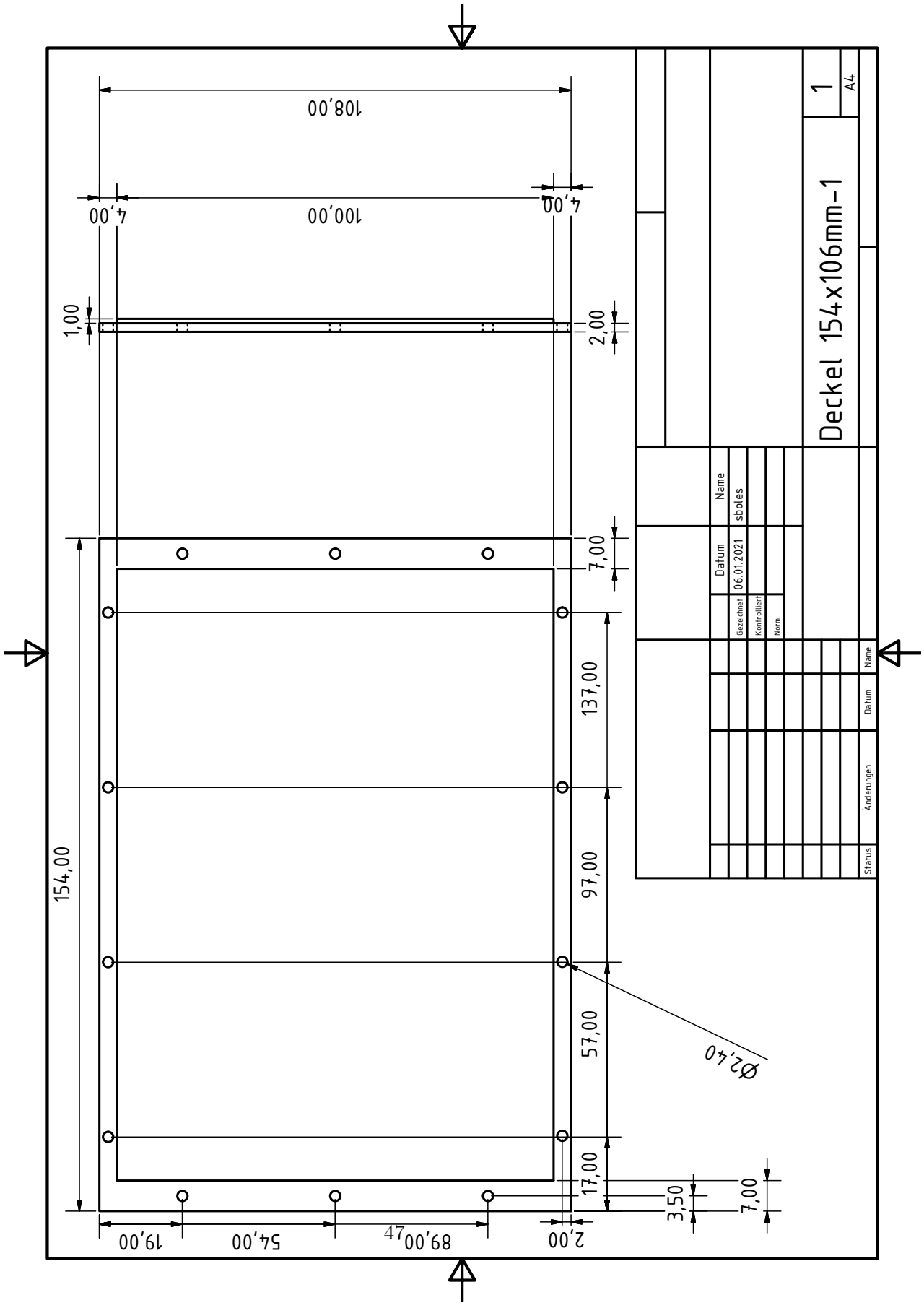
Deckel 154x106mm-1
A4
1
Name
sboles
Datum
06.01.2021
Gezeichnet
Kontrolliert
Norm
Status
Änderungen
Datum
Name
108,00
100,00
4,00
4,00
1,00
2,00
7,00
154,00
137,00
97,00
57,00
17,00
3,50
7,00
Ø2,40
19,00
54,00
89,00
2,00

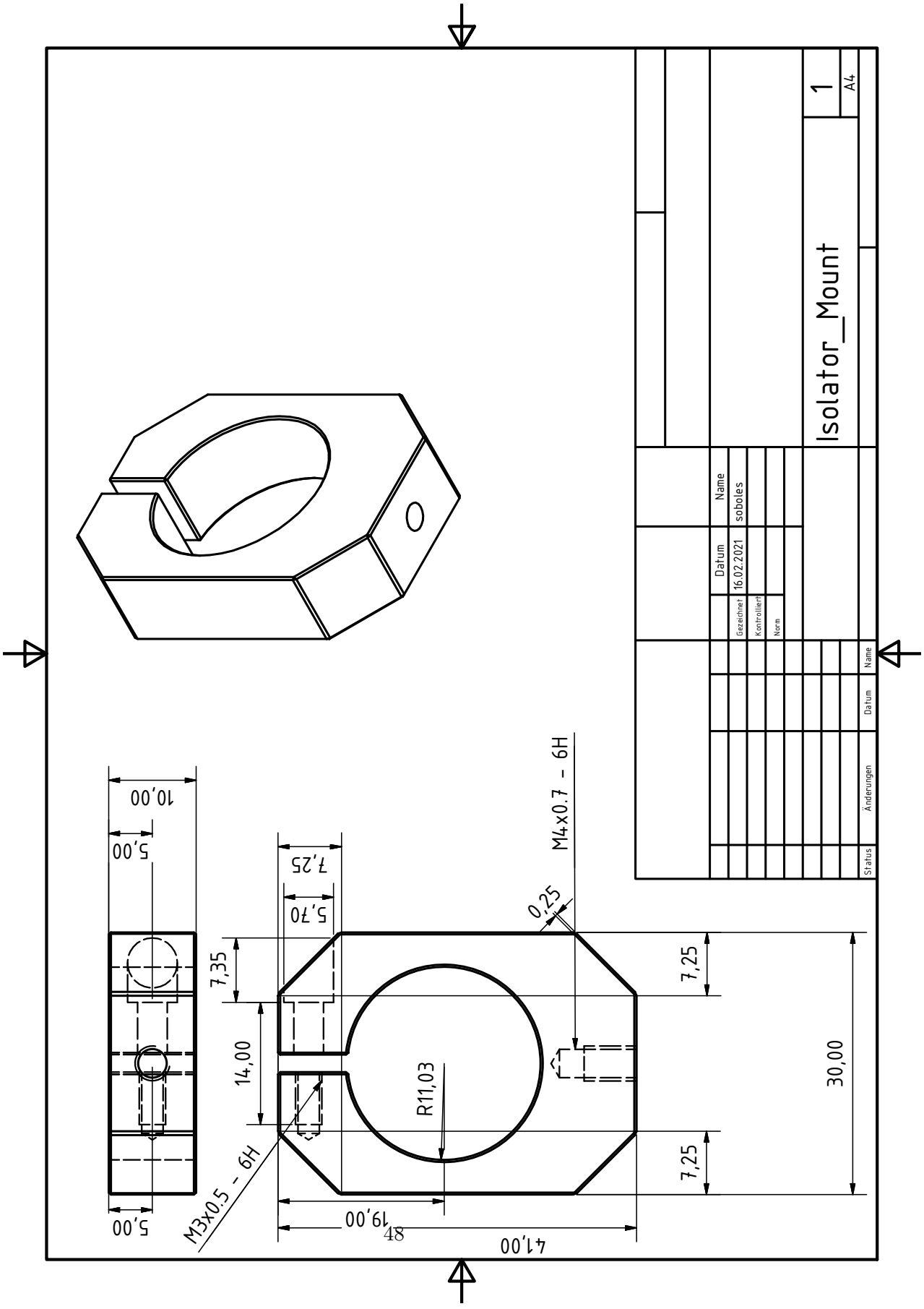
Isolator_Mount
1
A4
Name
soboles
Datum
16.02.2021
Gezeichnet
Kontrolliert
Norm
Status
Änderungen
Datum
Name
M4x0.7 - 6H
0,25
7,25
30,00
7,35
14,00
R11,03
M3x0.5 - 6H
19,00
41,00
5,70
7,25
10,00
5,00
5,00

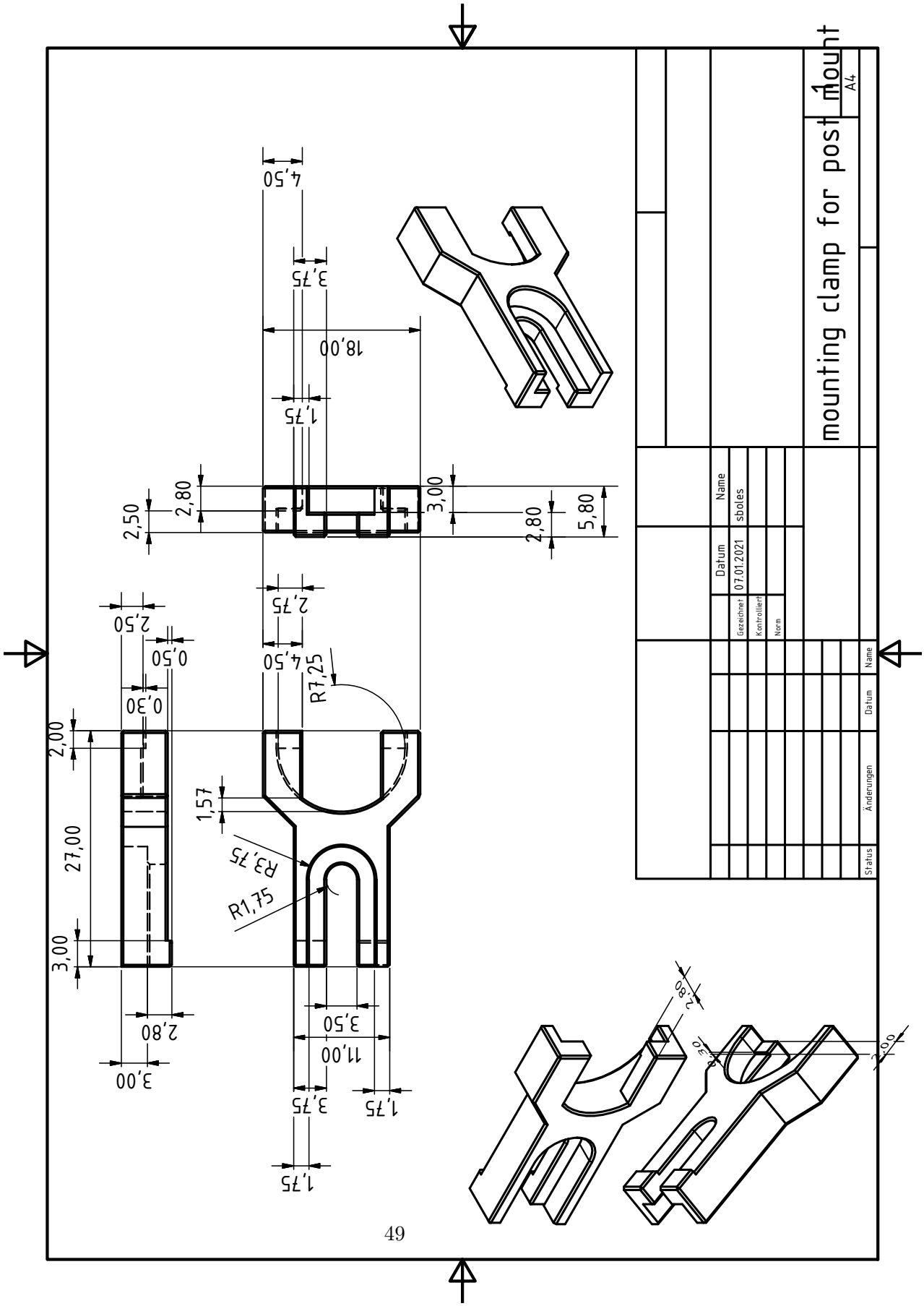
mounting clamp for post mount
A4
1
Name
sboles
Datum
07.01.2021
Gezeichnet
Kontrolliert
Norm
Status
Änderungen
Datum
Name
4,50
3,75
18,00
1,75
2,50
2,80
3,00
2,80
5,80
2,75
4,50
R7,25
2,50
0,50
0,30
2,00
27,00
3,00
1,57
R3,75
R1,75
2,80
3,50
11,00
3,75
1,75
3,00
1,75
2,80
2,00

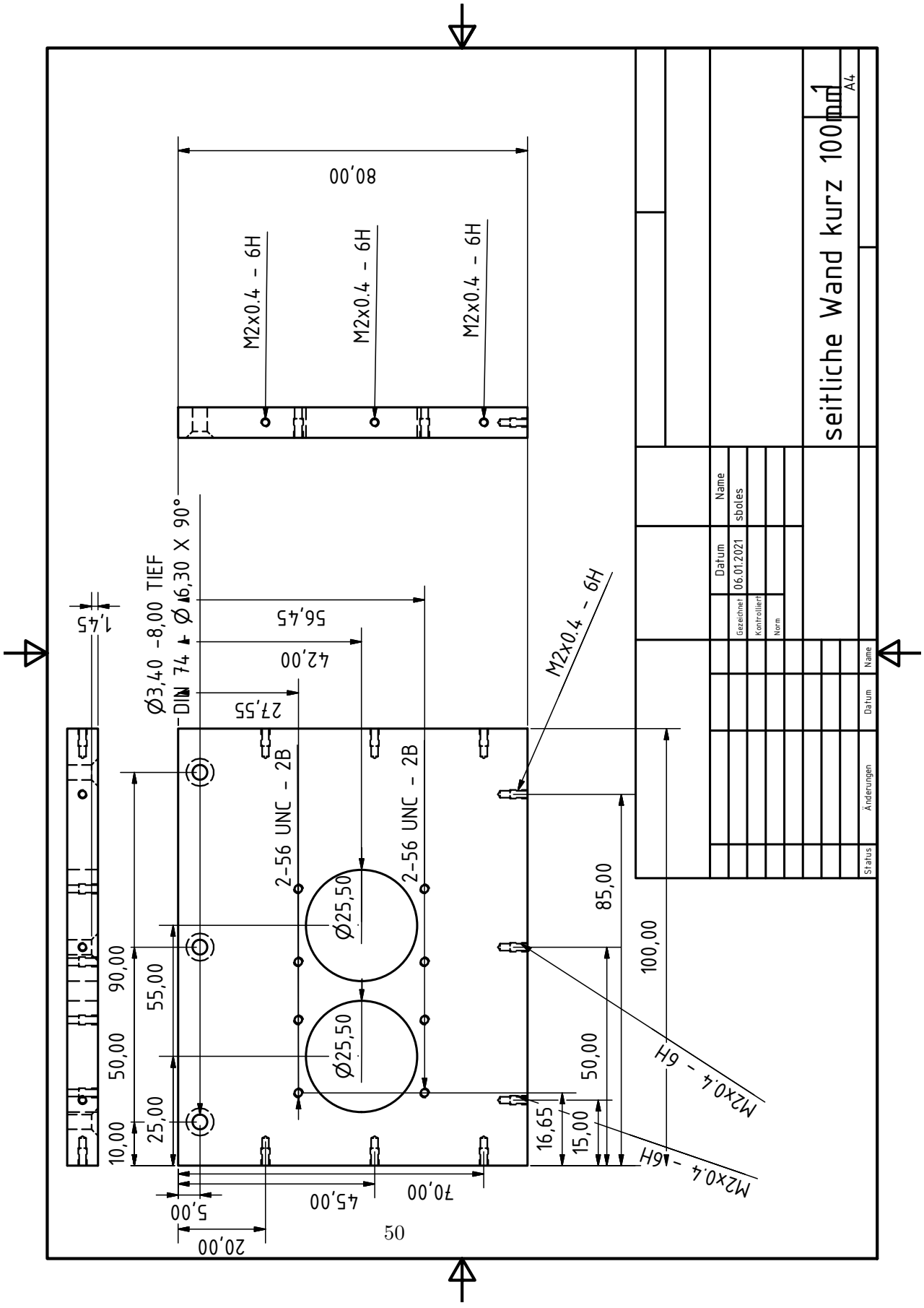
seitliche Wand kurz 100mm
A4
1
Name
Datum
sboles
06.01.2021
Gezeichnet
Kontrolliert
Norm
Status
Änderungen
Datum
Name
80,00
M2x0.4 - 6H
M2x0.4 - 6H
M2x0.4 - 6H
Ø3,40 -8,00 TIEF
DIN 74 - Ø6,30 X 90°
1,45
56,45
42,00
27,55
2-56 UNC - 2B
2-56 UNC - 2B
Ø25,50
Ø25,50
M2x0.4 - 6H
M2x0.4 - 6H
M2x0.4 - 6H
85,00
100,00
50,00
16,65
15,00
90,00
55,00
50,00
25,00
10,00
70,00
45,00
5,00
20,00

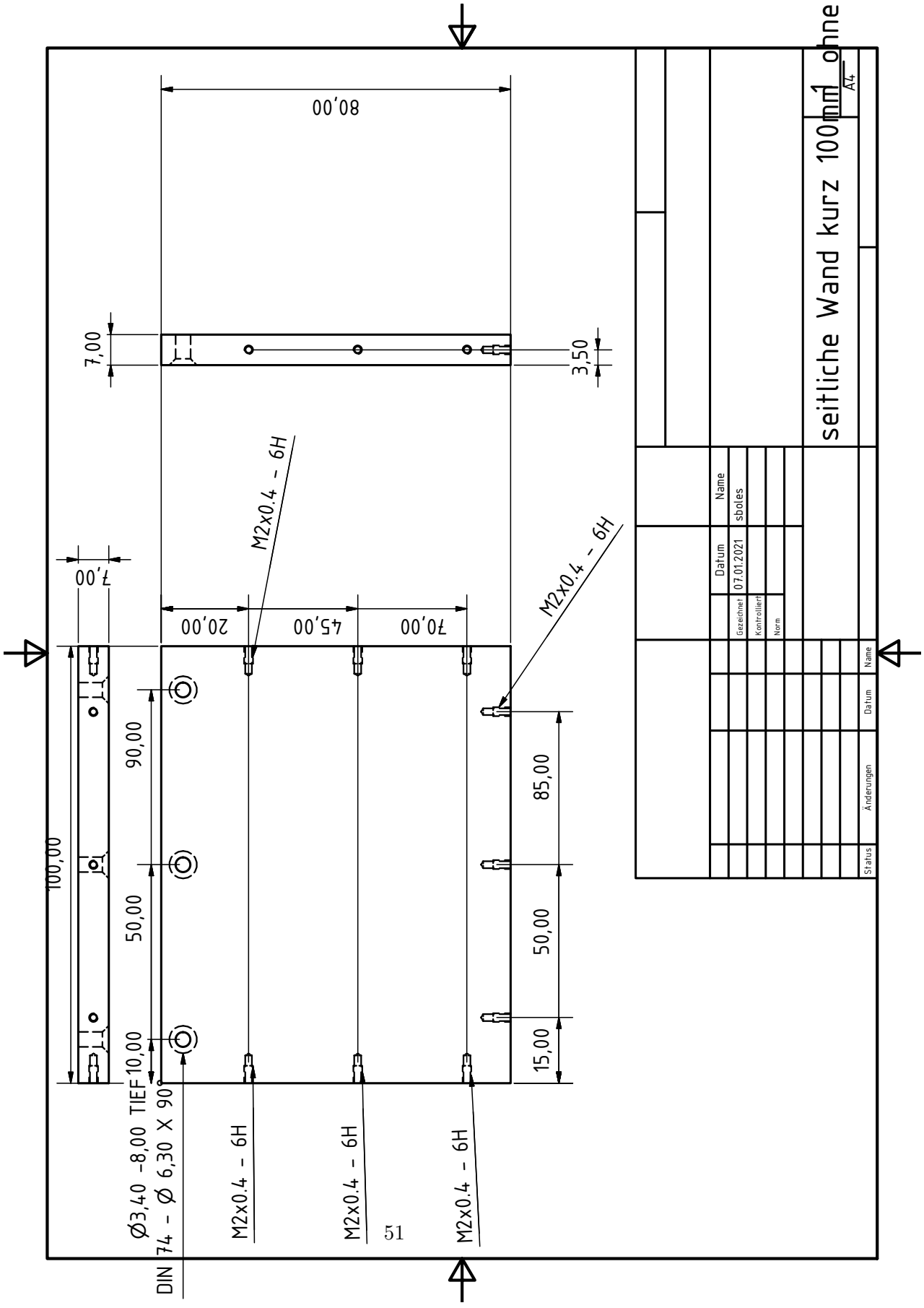
seitliche Wand kurz 100mm ohne
A4
Name
Datum
Gezeichnet
07.01.2021
sboles
Kontrolliert
Norm
Status
Änderungen
Datum
Name
80,00
7,00
3,50
M2x0.4 - 6H
M2x0.4 - 6H
7,00
20,00
45,00
70,00
100,00
90,00
50,00
10,00
85,00
50,00
15,00
Ø3,40 -8,00 TIEF
74 - Ø 6,30 X 90°
DIN
M2x0.4 - 6H
M2x0.4 - 6H
M2x0.4 - 6H

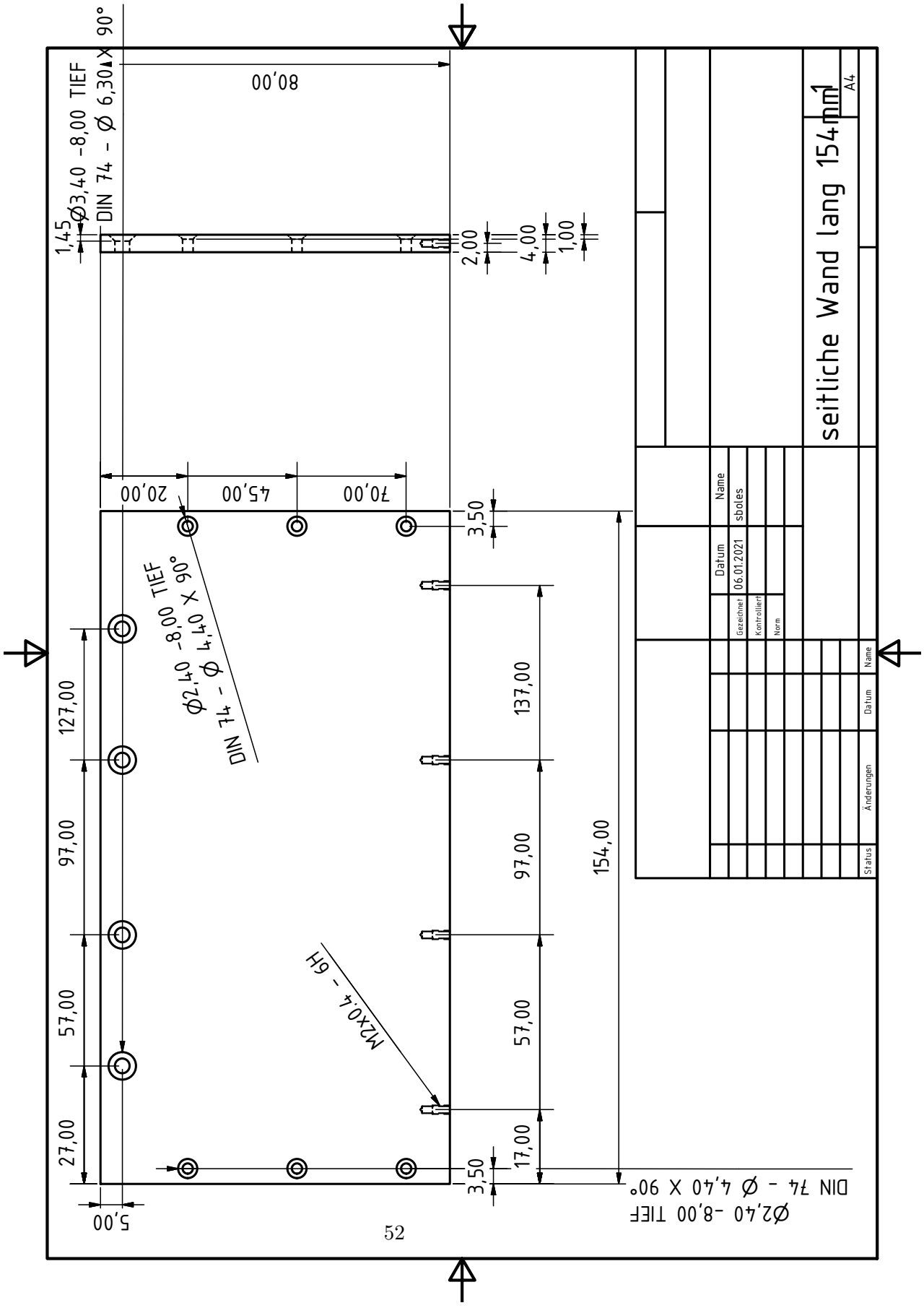
seitliche Wand lang 154mm
A4
Name
sboles
Datum
06.01.2021
Gezeichnet
Kontrolliert
Norm
Status
Änderungen
Datum
Name
80,00
Ø3,40 -8,00 TIEF
DIN 74 - Ø 6,30 X 90°
1,45
2,00
4,00
1,00
20,00
45,00
70,00
3,50
Ø2,40 -8,00 TIEF
DIN 74 - Ø 4,40 X 90°
127,00
97,00
57,00
27,00
137,00
97,00
57,00
17,00
154,00
M2X0,4 - 6H
5,00

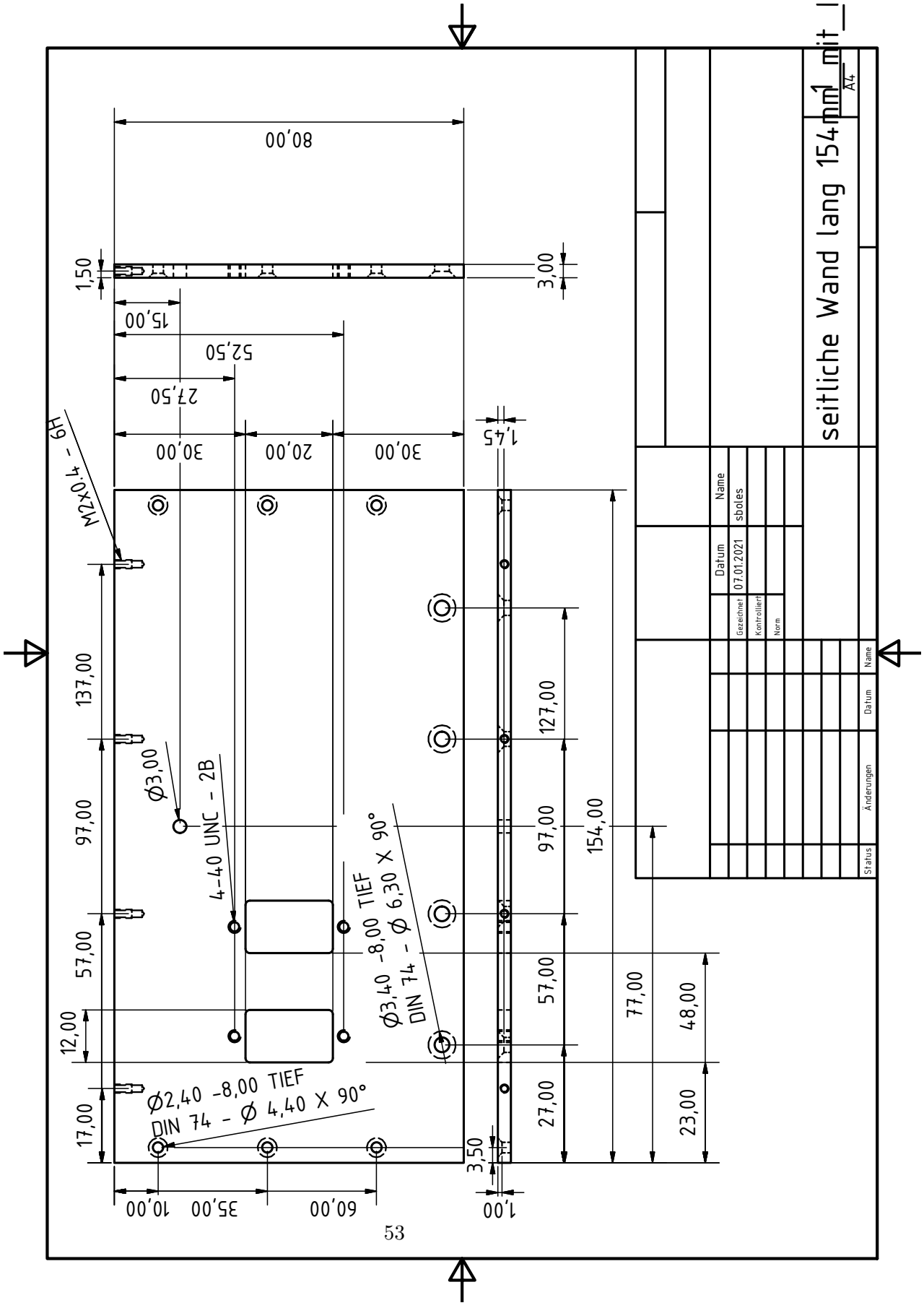
seitliche Wand lang 154mm mit _
A4
Name
sboles
Datum
07.01.2021
Gezeichnet
Kontrolliert
Norm
Status
Änderungen
Datum
Name
80,00
1,50
3,00
15,00
52,50
27,50
30,00
20,00
30,00
1,45
M2x0.4 - 6H
137,00
97,00
57,00
12,00
17,00
Ø3,00
4-40 UNC - 2B
Ø3,40 -8,00 TIEF
DIN 74 - Ø 6,30 X 90°
Ø2,40 -8,00 TIEF
DIN 74 - Ø 4,40 X 90°
127,00
97,00
57,00
27,00
154,00
77,00
48,00
23,00
3,50
1,00
10,00
35,00
60,00

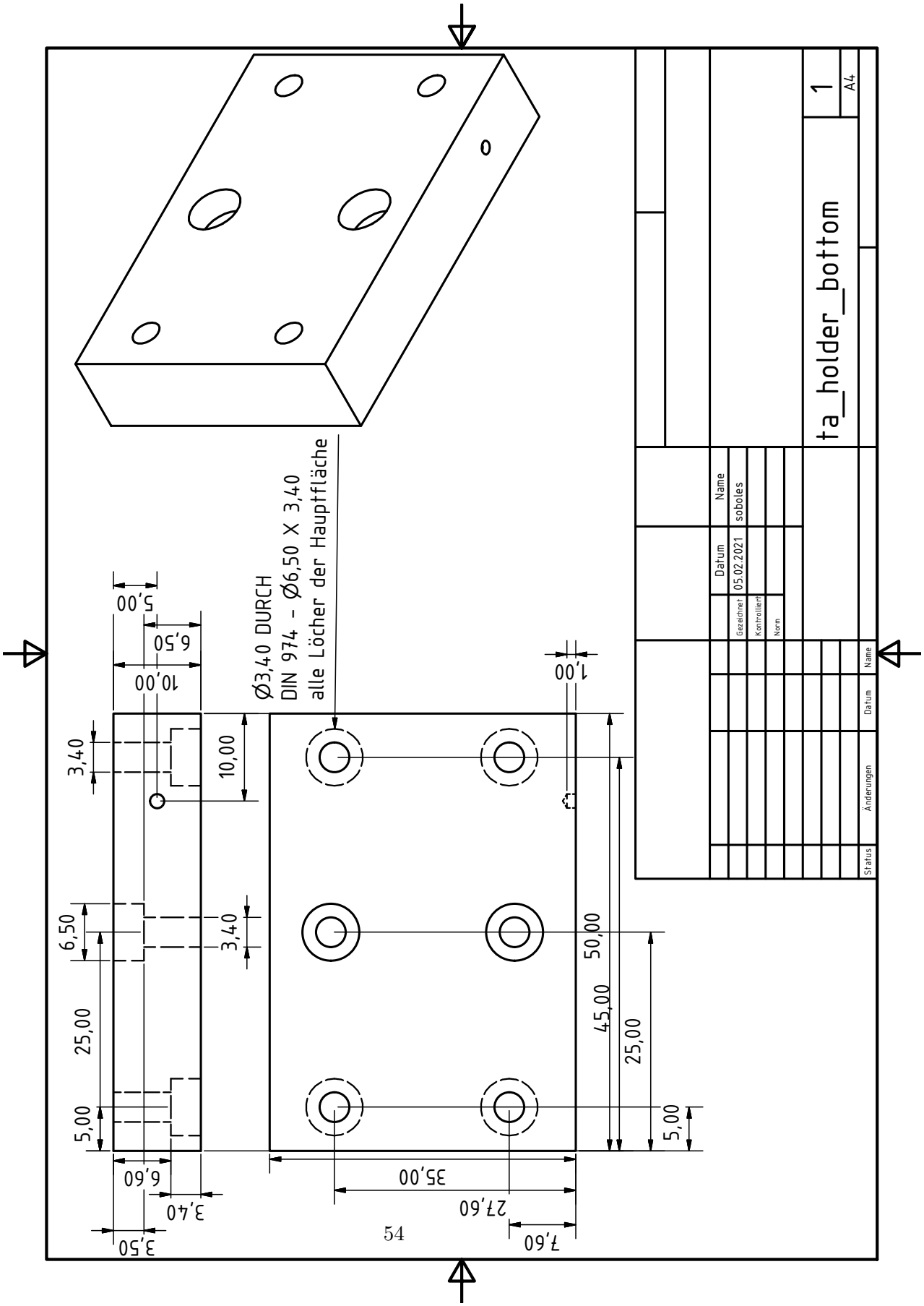
ta_holder_bottom
1
A4
Name
soboles
Datum
05.02.2021
Gezeichnet
Kontrolliert
Norm
Status
Änderungen
Datum
Name
Ø3,40 DURCH
DIN 974 - Ø6,50 X 3,40
alle Löcher der Hauptfläche
5,00
6,50
10,00
1,00
3,40
10,00
6,50
3,40
25,00
5,00
50,00
45,00
25,00
5,00
6,60
3,40
3,50
35,00
27,60
7,60

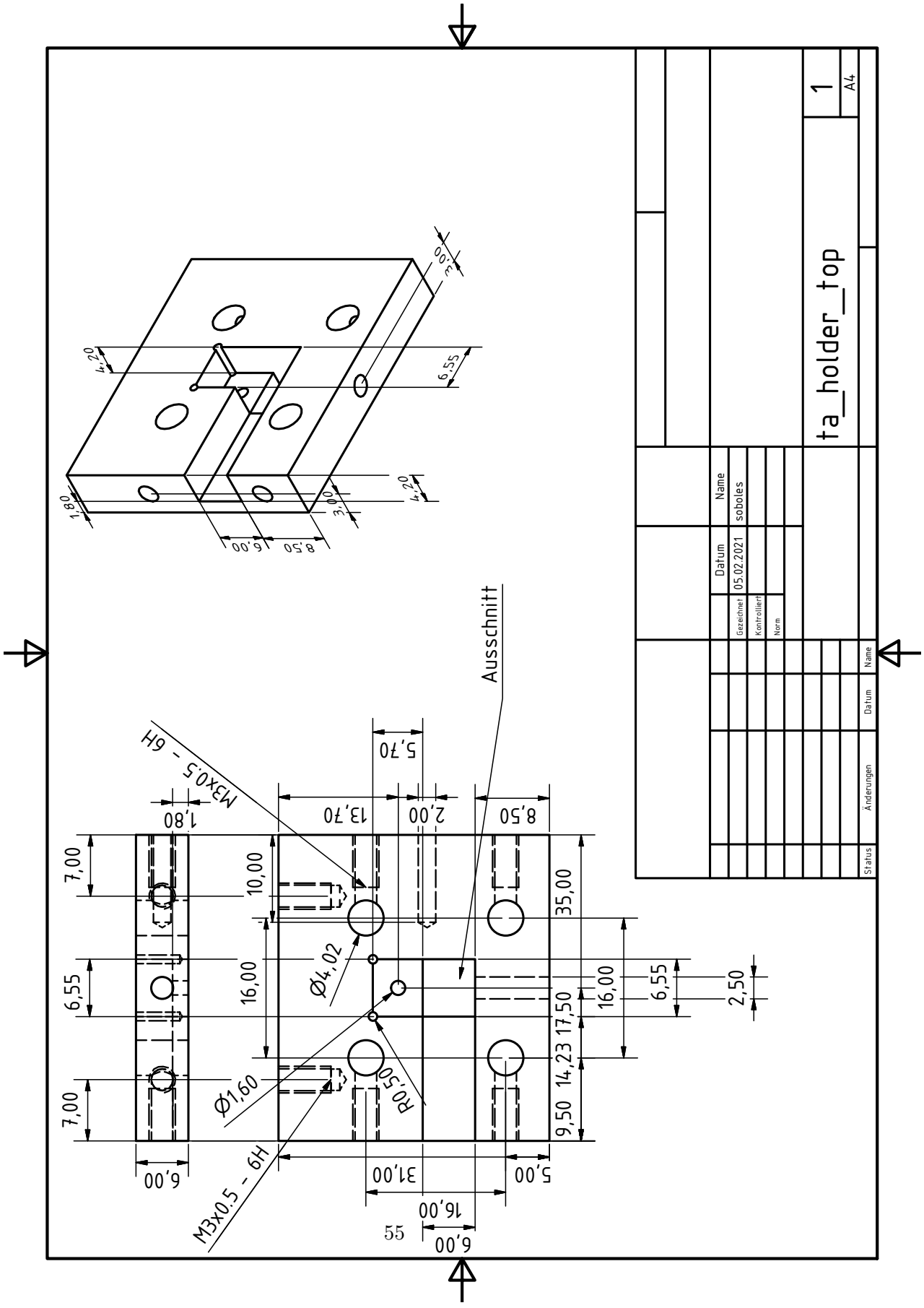
ta_holder_top
1
A4
Name
soboles
Datum
05.02.2021
Gezeichnet
Kontrolliert
Norm
Status
Änderungen
Datum
Name
Ausschnitt
M3x0.5 - 6H
M3x0.5 - 6H
Ø4,02
Ø1,60
R0,50
1,80
5,70
13,70
2,00
8,50
7,00
10,00
35,00
6,55
16,00
17,50
16,00
6,55
2,50
7,00
9,50
14,23
6,00
31,00
5,00
16,00
6,00
4,20
6,55
1,80
3,00
4,20
8,50
6,00
3,00